

AEDC-TR-74-80

Fig 1

**ARCHIVE COPY  
DO NOT LOAN**



**EXPERIMENTAL VERIFICATION OF A TRANSONIC TEST  
TECHNIQUE FOR FULL-SCALE INLET/ENGINE SYSTEMS  
SIMULATING MANEUVERING ATTITUDES**

R. L. Palko  
ARO, Inc.

PROPULSION WIND TUNNEL FACILITY  
ARNOLD ENGINEERING DEVELOPMENT CENTER  
AIR FORCE SYSTEMS COMMAND  
ARNOLD AIR FORCE STATION, TENNESSEE 37389

October 1974

Final Report for Period July 1, 1973 – June 30, 1974

Approved for public release; distribution unlimited.

Propulsion Wing, Air Force  
Arnold AFB  
F40000-75-0-0301

Prepared for

DIRECTORATE OF TECHNOLOGY (DY)  
ARNOLD ENGINEERING DEVELOPMENT CENTER  
ARNOLD AIR FORCE STATION, TN 37389

AEDC TECHNICAL LIBRARY



5 0720 00033 7339

## NOTICES

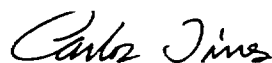
When U. S. Government drawings specifications, or other data are used for any purpose other than a definitely related Government procurement operation, the Government thereby incurs no responsibility nor any obligation whatsoever, and the fact that the Government may have formulated, furnished, or in any way supplied the said drawings, specifications, or other data, is not to be regarded by implication or otherwise, or in any manner licensing the holder or any other person or corporation, or conveying any rights or permission to manufacture, use, or sell any patented invention that may in any way be related thereto.

Qualified users may obtain copies of this report from the Defense Documentation Center.

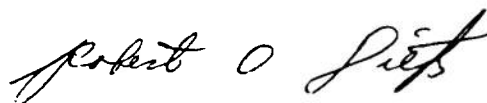
References to named commercial products in this report are not to be considered in any sense as an endorsement of the product by the United States Air Force or the Government.

## APPROVAL STATEMENT

This technical report has been reviewed and is approved.



CARLOS TIRRES  
Captain, USAF  
Research and Development  
Division  
Directorate of Technology



ROBERT O. DIETZ  
Director of Technology

# UNCLASSIFIED

REPORT DOCUMENTATION PAGE		READ INSTRUCTIONS BEFORE COMPLETING FORM
1. REPORT NUMBER <b>AEDC-TR-74-80</b>	2. GOVT ACCESSION NO.	3. RECIPIENT'S CATALOG NUMBER
4. TITLE (and Subtitle) <b>EXPERIMENTAL VERIFICATION OF A TRANSONIC TEST TECHNIQUE FOR FULL-SCALE INLET/ENGINE SYSTEMS SIMULATING MANEUVERING ATTITUDES</b>		5. TYPE OF REPORT & PERIOD COVERED <b>Final Report, July 1, 1973 to June 30, 1974</b>
		6. PERFORMING ORG. REPORT NUMBER
7. AUTHOR(s) <b>R. L. Palko, ARO, Inc.</b>		8. CONTRACT OR GRANT NUMBER(s)
9. PERFORMING ORGANIZATION NAME AND ADDRESS <b>Arnold Engineering Development Center Arnold Air Force Station, TN 37389</b>		10. PROGRAM ELEMENT, PROJECT, TASK AREA & WORK UNIT NUMBERS <b>Program Element 65802F</b>
11. CONTROLLING OFFICE NAME AND ADDRESS <b>Arnold Engineering Development Center (DYFS) Arnold Air Force Station, TN 37389</b>		12. REPORT DATE <b>October 1974</b>
		13. NUMBER OF PAGES <b>34</b>
14. MONITORING AGENCY NAME & ADDRESS (if different from Controlling Office)		15. SECURITY CLASS. (of this report) <b>UNCLASSIFIED</b>
		15a. DECLASSIFICATION DOWNGRADING SCHEDULE <b>N/A</b>
16. DISTRIBUTION STATEMENT (of this Report) <b>Approved for public release; distribution unlimited.</b>		
17. DISTRIBUTION STATEMENT (of the abstract entered in Block 20, if different from Report) <i>in inlet testing</i>		
18. SUPPLEMENTARY NOTES  <b>Available in DDC.</b>		
19. KEY WORDS (Continue on reverse side if necessary and identify by block number) <b>airbreathing propulsion inlets inlet air pressure transonic wind tunnels airframe-propulsion compatibility airframe-propulsion system integration</b>		
20. ABSTRACT (Continue on reverse side if necessary and identify by block number) <b>An experimental investigation was conducted to demonstrate the capability of a newly developed flow-shaping technique to test full-scale inlet/engine systems in the AEDC 16-ft Propulsion Wind Tunnel (transonic) at angles of yaw and combinations of angle of attack and yaw. Simulation of the flow field approaching the inlet was accomplished at Mach numbers in the range from 0.6 to 0.9 at positive yaw angles up to 6 deg over an angle-of-attack range from</b>		

## UNCLASSIFIED

## UNCLASSIFIED

20, Continued

0 to 8 deg and at negative yaw angles up to 6 deg over an angle of attack range from 0 to 12 deg. Inlet pressure distribution (ramp, lip, and sideplate), local flow angularity, and local Mach number in front of the inlet were used to verify the technique. The base data to be verified were obtained in the AEDC 4-ft Aerodynamic Wind Tunnel (transonic) with a fuselage/inlet model. The data were verified in the AEDC 1-ft Aerodynamic Wind Tunnel (transonic) using a 1/16-scale model with the flow-shaping devices.

UNCLASSIFIED

## PREFACE

The work reported herein was conducted by the Arnold Engineering Development Center (AEDC), Air Force Systems Command (AFSC), under Program Element 65802F. The technical monitoring of the effort was performed by Capt. Carlos Tirres, USAF, Research and Development Division, Directorate of Technology. The results presented were obtained by ARO, Inc. (a subsidiary of Sverdrup & Parcel and Associates, Inc.), contract operator of AEDC, AFSC, Arnold Air Force Station, Tennessee. The investigation was conducted under ARO Project Nos. PF418 and PA428. The manuscript (ARO Control No. ARO-PWT-TR-74-51) was submitted for publication on June 24, 1974.

Acknowledgement is made of the contributions of Mr. W. P. Harman of the Propulsion Wind Tunnel Facility, Test Operations Branch, who designed the test equipment, and Dr. M. D. High, Supervisor, Analysis Section, Propulsion Wind Tunnel Facility, 16T/S Projects Branch, who supported the research effort from its beginning.

## CONTENTS

	<u>Page</u>
1.0 INTRODUCTION . . . . .	5
2.0 EXPERIMENTAL VERIFICATION OF SIMULATION TECHNIQUE . . . . .	5
3.0 APPARATUS	
3.1 Wind Tunnels . . . . .	8
3.2 Inlet Model . . . . .	10
3.3 Flow Angularity Probe . . . . .	11
3.4 Flow-Shaping Devices . . . . .	13
3.5 Instrumentation and Data Acquisition Systems . . . . .	14
4.0 RESULTS AND DISCUSSION . . . . .	15
5.0 CONCLUSIONS . . . . .	32
REFERENCES . . . . .	32

## ILLUSTRATIONS

### Figure

1. Fuselage and Inlet/Engine Configuration Installed in PWT-4T . . . . .	6
2. Installation of Inlet Model and Flow-Shaping Device in PWT-1T during Pitch-Yaw Simulation . . . . .	7
3. Schematic of PWT-4T Test Section with Fuselage/Inlet Model Installed . . . . .	8
4. General Arrangement of the PWT-1T and Supporting Equipment . . . . .	9
5. Schematic of the PWT-1T Test Leg . . . . .	10
6. Inlet Model Configurations and Pressure Orifice Locations . . . . .	11
7. Flow Angularity Probe and Calibration Support Mechanism . . . . .	12
8. Schematic of the Model Installation in the PWT-1T . . . . .	12
9. Schematic of Flow-Shaping Device . . . . .	13
10. Model and Cylinder Positioning Mechanism Installed in PWT-1T . . . . .	14
11. Effect of Changes in MFR on Inlet Surface Pressure Distribution at $\alpha = 0$ and $\psi = 0$ . . . . .	16
12. Effect of Changes in Unit Reynolds Number in PWT-4T on the Inlet Surface Pressure Distribution at $\alpha = 4$ deg and $\psi = -4$ deg . . . . .	17
13. Local Upwash and Sidewash Angles in Front of the Inlet as a Function of Aircraft Pitch and Yaw Angles . . . . .	20
14. Local Mach Number in Front of the Inlet as a Function of Aircraft Pitch and Yaw Angles . . . . .	24

<u>Figure</u>	<u>Page</u>
15. Comparison of Inlet Surface Pressure Distribution for Actual and Simulated Yaw and Pitch-Yaw Combinations at a Mach Number of 0.6 . . . . .	25
16. Comparison of Inlet Surface Pressure Distribution for Actual and Simulated Yaw and Pitch-Yaw Combinations at a Mach Number of 0.7 . . . . .	26
17. Comparison of Inlet Surface Pressure Distribution for Actual and Simulated Yaw and Pitch-Yaw Combinations at a Mach Number of 0.8 . . . . .	27
18. Comparison of Inlet Surface Pressure Distribution for Actual and Simulated Yaw and Pitch-Yaw Combinations at a Mach Number of 0.9 . . . . .	28
19. Comparison of Inlet Surface Pressure Distribution for Actual and Simulated Pitch Angles . . . . .	29
20. Effect of Change in MFR on Inlet Surface Pressure Distribution . . . . .	30
21. Typical Performance for Highly Maneuverable Aircraft and Full-Scale Inlet/Engine Testing Capability of the PWT-16T . . . . .	31

**TABLE**

1. Tabulated PWT-1T, Inlet Model, and Shaping Device Settings for Flow Simulation . . . . .	19
 NOMENCLATURE . . . . .	 33

## 1.0 INTRODUCTION

Full-scale inlet/engine systems testing has been a part of the AEDC mission since the completion of the AEDC 16-ft Propulsion Wind Tunnels. However, high angle-of-attack testing capability and a capability to test at angles of yaw or combinations of angle of attack and yaw have never existed. The requirement for additional test capability has increased as the maneuvering performance envelope of aircraft has increased, whereas the ground facility testing capability has remained static. Inlet/engine compatibility problems encountered during the development of some recent high performance aircraft have shown that the gap between the aircraft maneuvering envelope and the present testing capability has grown too large.

In an effort to decrease this gap a study was undertaken in January 1971 to develop a new testing technique and to produce criteria for the modification of the AEDC Propulsion Wind Tunnel Facility (PWT) 16-ft Propulsion Wind Tunnel (transonic) (PWT-16T) that together would provide a broader capability to test full-scale inlet/engine systems for highly maneuverable aircraft. The goal of the study was to provide angles of attack up to 25 deg and angles of yaw up to  $\pm 5$  deg. The study was basically made in three phases. The first phase was the development of flow-shaping devices which would give a desired flow-field simulation, and the results are reported in Refs. 1, 2, and 3. The second phase was the experimental verification of the high angle-of-attack simulation capability of the technique with an inlet model, and the results are reported in Ref. 4. The third phase was the experimental verification of yaw and combination of angle-of-attack and yaw simulation capability of the technique which is reported herein.

## 2.0 EXPERIMENTAL VERIFICATION OF THE SIMULATION TECHNIQUE

The method used to verify the inlet flow simulation capability of the flow-shaping technique was to first obtain experimental data with the inlet/engine simulation model (inlet model) at several geometric angles of yaw and combinations of angle of attack and yaw. When angle of attack was simulated alone (Ref. 4), the base data were obtained in the AEDC 1-ft Aerodynamic Wind Tunnel (transonic) (PWT-1T) with a 1/16-scale inlet model with a partial forebody. However, to obtain the base data for simulation with yaw angles it was necessary to have a complete fuselage forward of the inlet. With a complete fuselage the model was too large for the 1-ft tunnel, so the base data were obtained in the AEDC 4-ft Aerodynamic Wind Tunnel (transonic) (PWT-4T). The installation of the fuselage model in PWT-4T is shown in Fig. 1. After the base data were obtained, these data were duplicated in PWT-1T using the inlet model with a partial forebody and the flow-shaping devices. The installation of the inlet model in Tunnel 1T with one flow-shaping configuration is shown in Fig. 2.



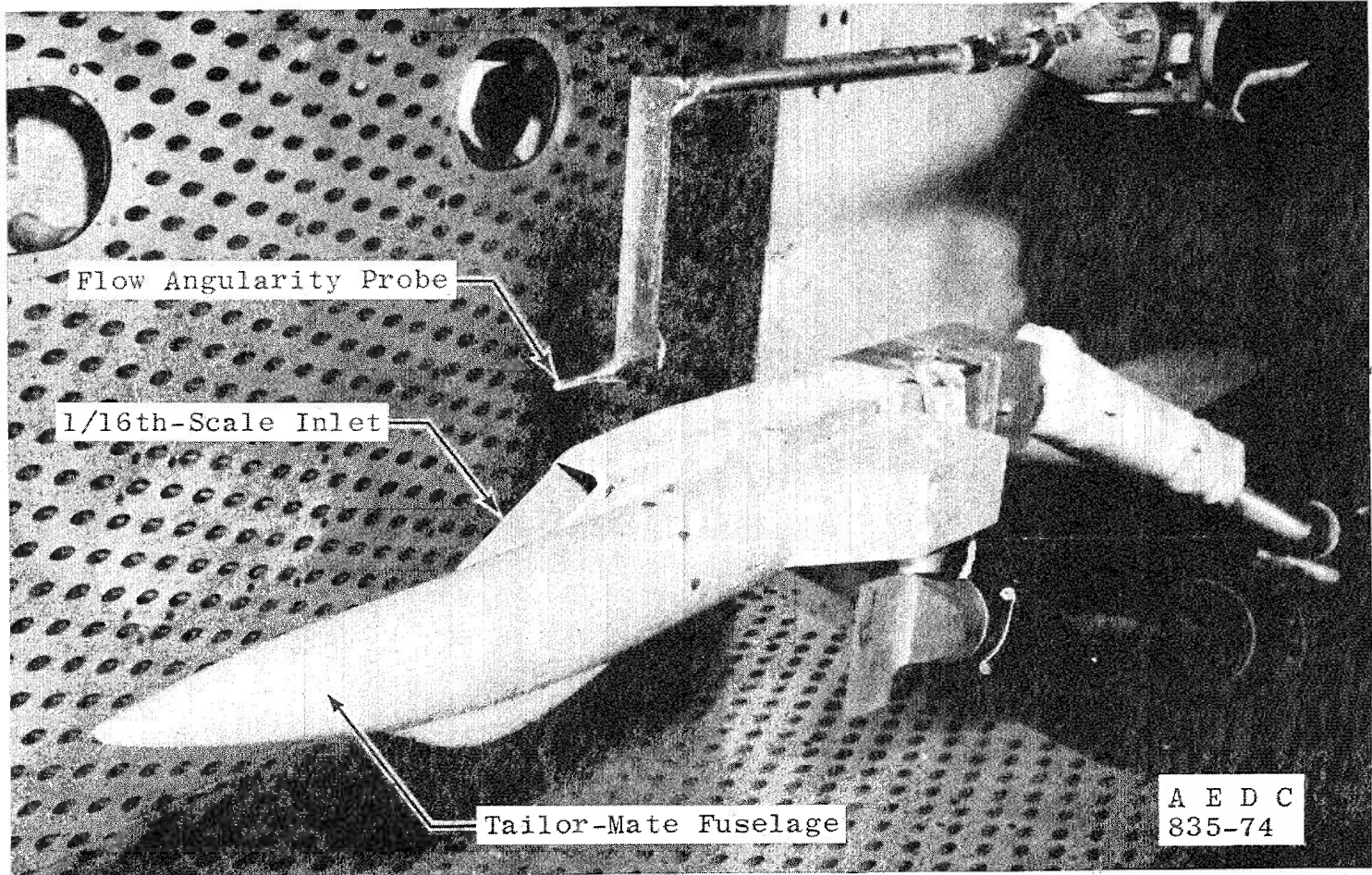


Figure 1. Fuselage and inlet/engine configuration installed in PWT-4T.

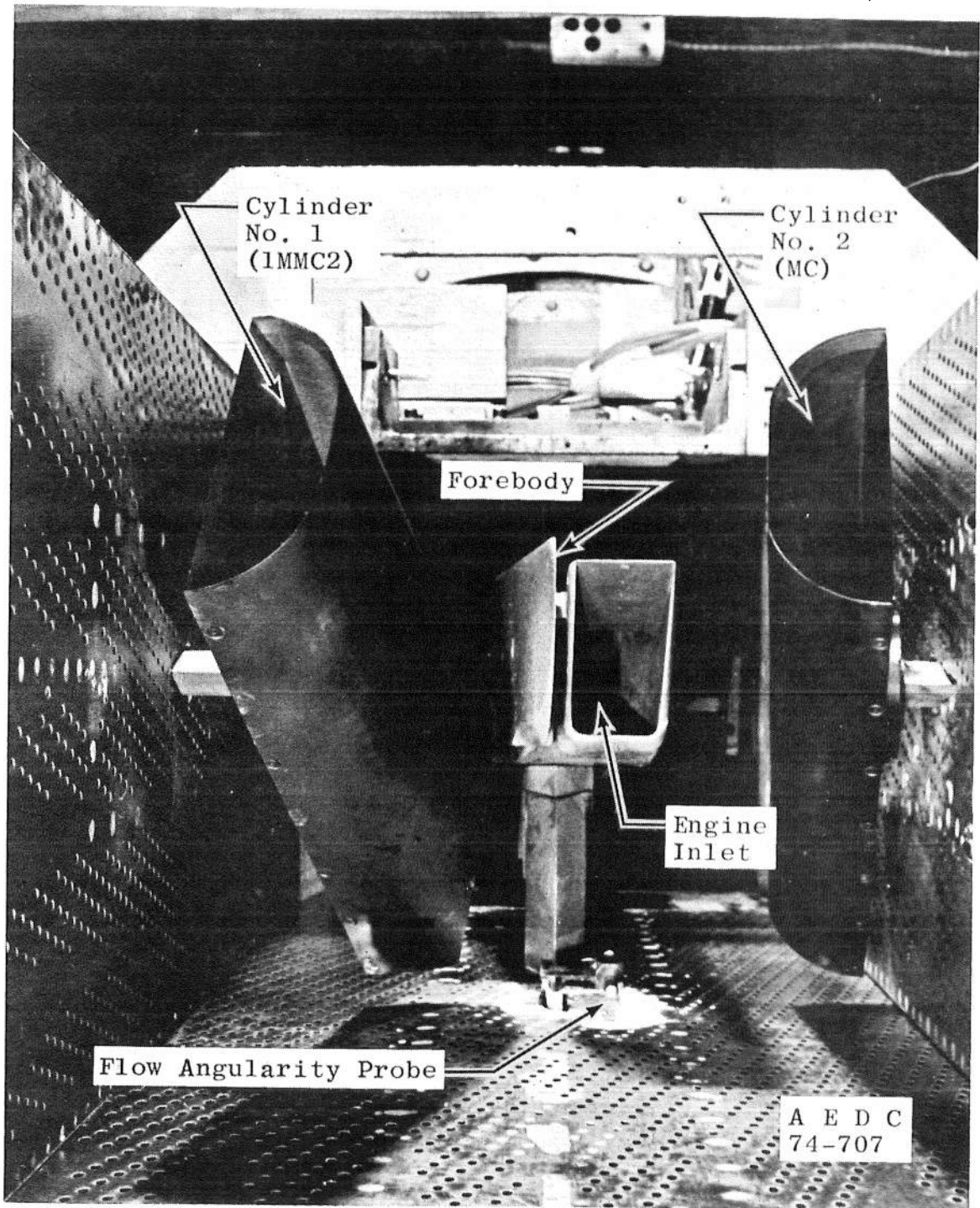


Figure 2. Installation of inlet model and flow-shaping device in PWT-1T during pitch-yaw simulation.

Matching of the pressure distribution on the inlet ramp, lip, and sideplates along with the measured local flow angularity and Mach number in front of the inlet was used as a basis for proof of inlet flow-field simulation. The inlet duct total and static pressures were also measured so that the mass flow ratio (MFR) could be duplicated between the Tunnel 1T and 4T experiments.

### 3.0 APPARATUS

#### 3.1 WIND TUNNELS

##### 3.1.1 AEDC PWT-4T

Tunnel 4T is a closed-loop, continuous flow, variable density tunnel in which the Mach number can be varied from 0.1 to 1.3. At all Mach numbers, the stagnation pressure can be varied from 300 to 3700 psfa. The test section is 4 ft square and 12.5 ft long with perforated, variable porosity (0.5- to 10-percent open) walls. It is completely enclosed in a plenum chamber from which the air can be evacuated, allowing part of the tunnel airflow to be removed through the perforated walls of the test section. A sketch of the test section wall details and location of the inlet/fuselage model in the test section is shown in Fig. 3.

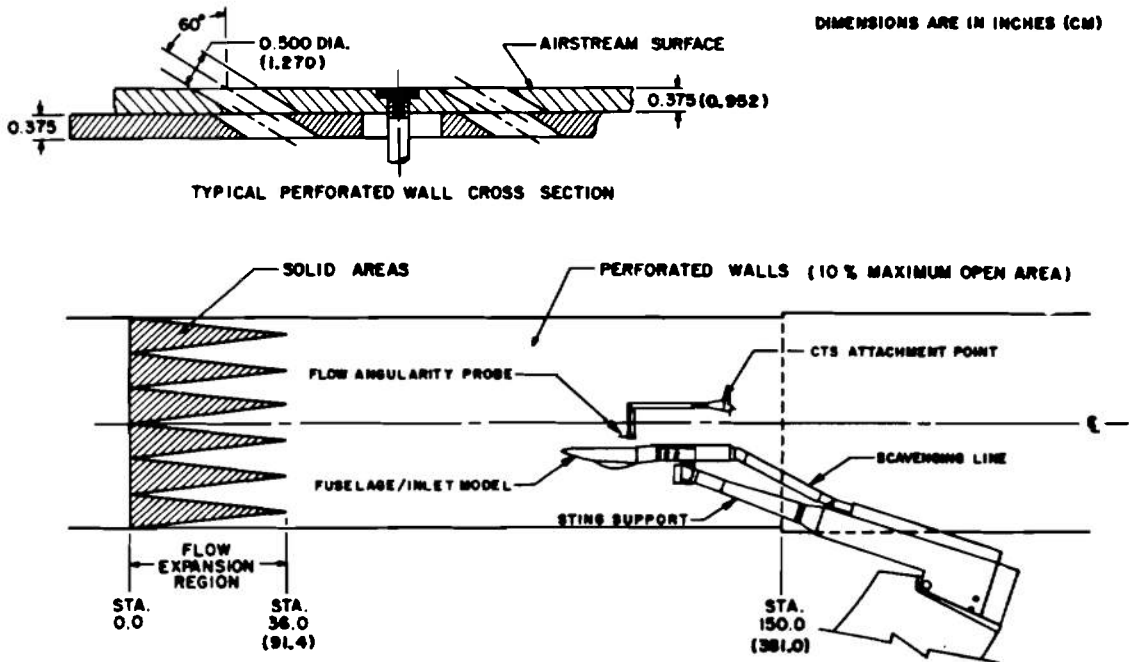


Figure 3. Schematic of PWT-4T test section with fuselage/inlet model installed.

For flow angularity measurements, two separate and independent support systems were used. The fuselage/inlet model was inverted in the test section and supported by an offset sting attached to the main pitch sector. The flow angularity probe was supported by the Captive Trajectory Support (CTS), which extends down from the tunnel top wall and provides probe movement (six degrees of freedom) independent of the inlet model. This system allowed the probe to be positioned in front of the inlet to determine the local flow angularity and Mach number.

### 3.1.2 AEDC PWT-1T

Tunnel 1T is a continuous flow, nonreturn, transonic wind tunnel equipped with a two-dimensional, flexible nozzle and a plenum evacuation system. The test section Mach number range can normally be varied from 0.2 to 1.50. Total-pressure control is not available, and the tunnel is operated at a stilling chamber total pressure of about 2850 psfa with a  $\pm 5$ -percent variation depending on tunnel resistance and ambient conditions. The stagnation temperature can be varied from 80 to 120°F above ambient temperature when necessary to prevent moisture condensations in the test region.

The general arrangement of the tunnel and its associated equipment is shown in Fig. 4, and a schematic of the nozzle, test section, and wall geometry is shown in Fig. 5.

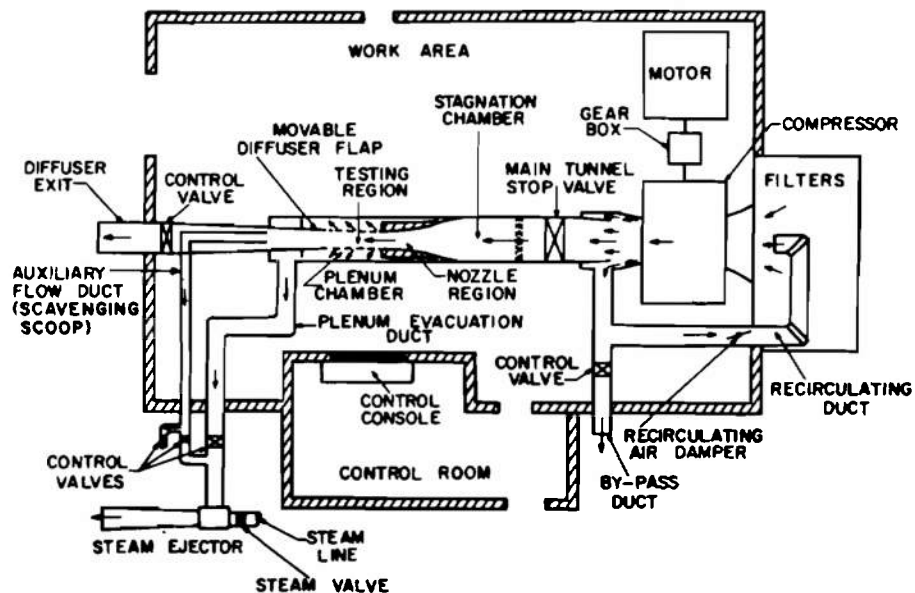


Figure 4. General arrangement of the PWT-1T and supporting equipment.

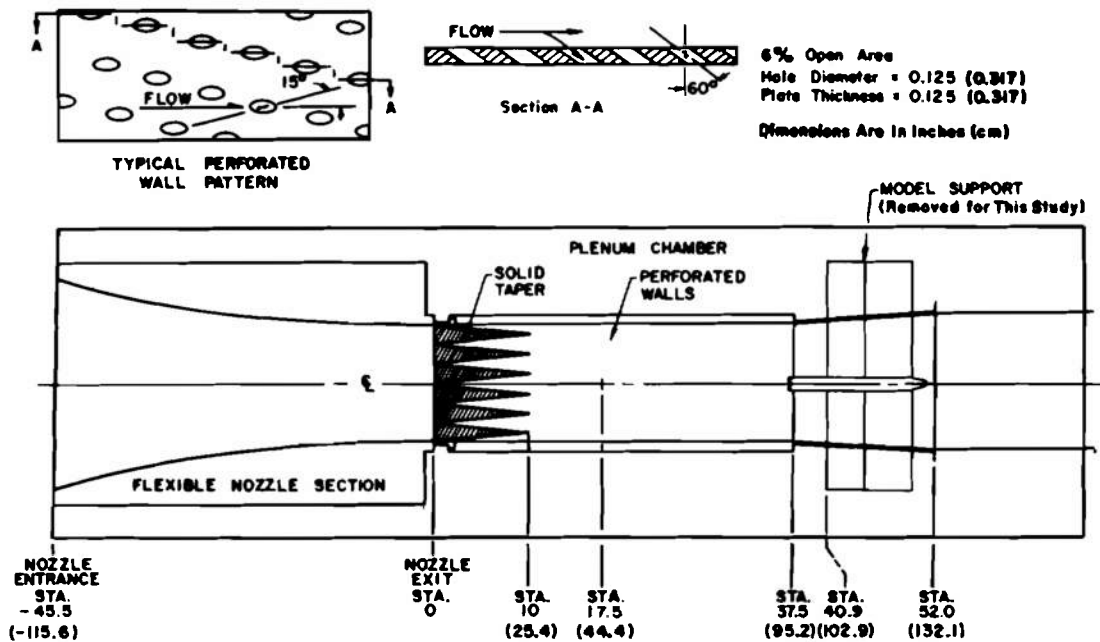


Figure 5. Schematic of the PWT-1T test leg.

### 3.2 INLET MODEL

The inlet model used was a 1/16-scale, two-dimensional, supersonic inlet available from a previous wind tunnel blockage study. This inlet model was also used in the angle-of-attack verification study reported in Ref. 4. Pressure orifices were located along the inlet ramp, lip, and sideplates in the positions shown in Fig. 6. The pressure measured at each of these orifices was used as one of the indicators of inlet flow-field simulation. A total pressure probe and static pressure orifice were located in the inlet duct near the engine-face station location to determine the MFR of the inlet.

To obtain the base data from PWT-4T a fuselage was fabricated to accommodate the 1/16-scale inlet blockage model. This fuselage was contoured as a subscale model of one of the Air Force Flight Dynamics Laboratory (AFFDL) Airframe/Propulsion Systems Integration (APSI) Tailor-Mate configurations which represented a typical high performance aircraft. The fuselage model was attached to the model support sting with a clutch face which allowed the model to be set in yaw at 2-deg increments. A scavenging line connected the inlet model duct to a small air ejector which was used to simulate engine airflow through the inlet. The model angle of attack was set with the main pitch sector.

To obtain the simulation data in PWT-1T a forebody was used with the 1/16-scale inlet. This forebody (designated N-1, see Fig. 6) had a very sharp edge along the front

and bottom to restrict the flow from turning toward the fuselage side of the inlet. The model could be manually positioned in the tunnel to place the center of the inlet on the tunnel centerline or 1 in. (2.54 cm) below the centerline. The model angle of attack could also be manually changed from 0 to 12 deg in 2-deg increments. Flow through the inlet was varied by a control valve in the scavenging scoop line to set the MFR.

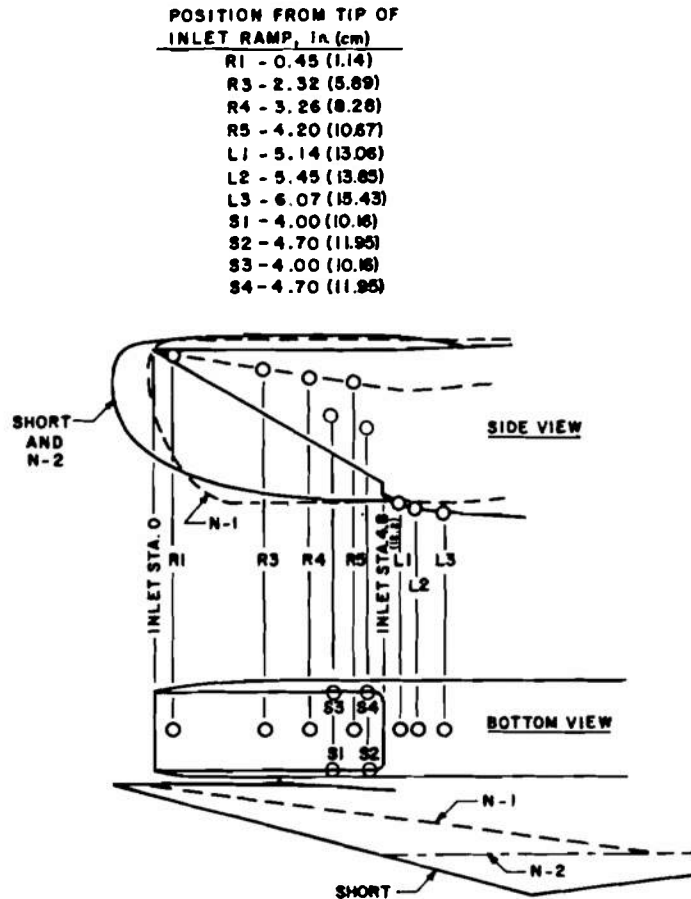


Figure 6. Inlet model configurations and pressure orifice locations.

### 3.3 FLOW ANGULARITY PROBE

A flow angularity probe was used to measure the local flow angularity and Mach number in front of the inlet. Details of the probe are shown in Fig. 7. (A discussion of the probe calibration and accuracy is given in Ref. 3.) A probe drive system was used to remotely position the probe from the tunnel wall to the tunnel centerline at a station where the probe tip was near the leading edge of the inlet ramp. The installation position of the probe is shown schematically in Fig. 8.

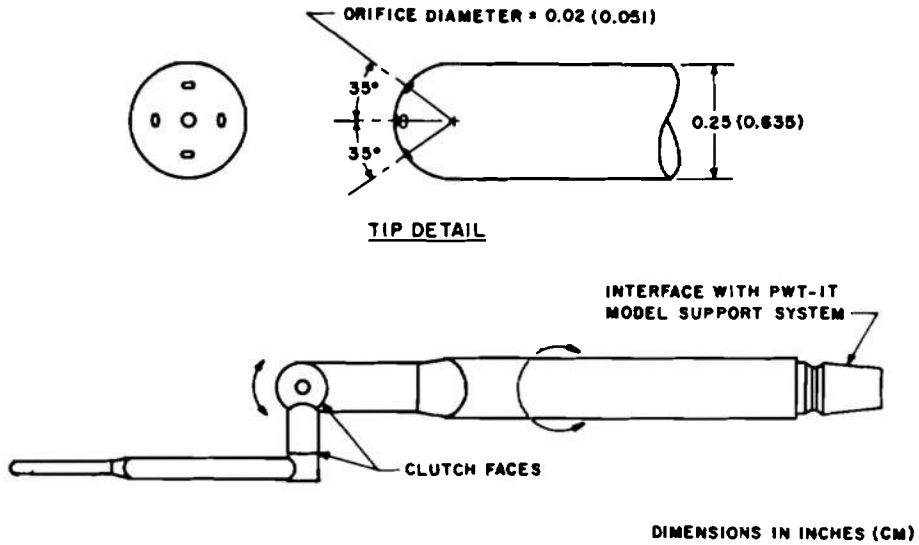


Figure 7. Flow angularity probe and calibration support mechanism.

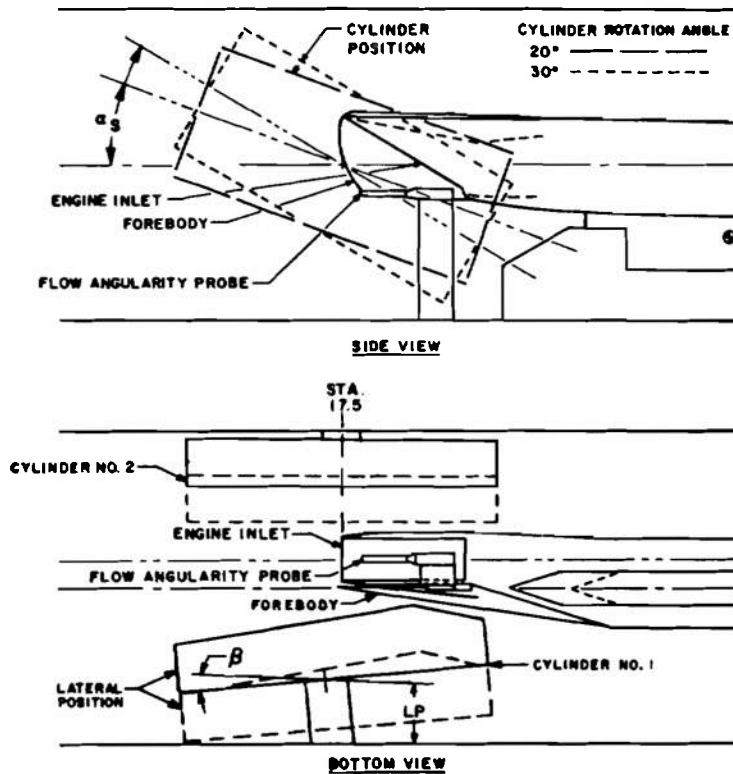


Figure 8. Schematic of the model installation in the PWT-1T.

### 3.4 FLOW-SHAPING DEVICES

The basic flow-shaping device consisted of two hollow, half-circular cylinders which were split and widened in the middle by the width of one radius. The general arrangement of the devices along with the inlet model is shown in Fig. 8. The dimensions and shape of the individual cylinders are given in Fig. 9a. Five variations of the base configuration were tried during the experiments, with the base configuration and three of the variations giving useful simulations in five combinations. These variations and the useful combinations are also shown in Fig. 9.

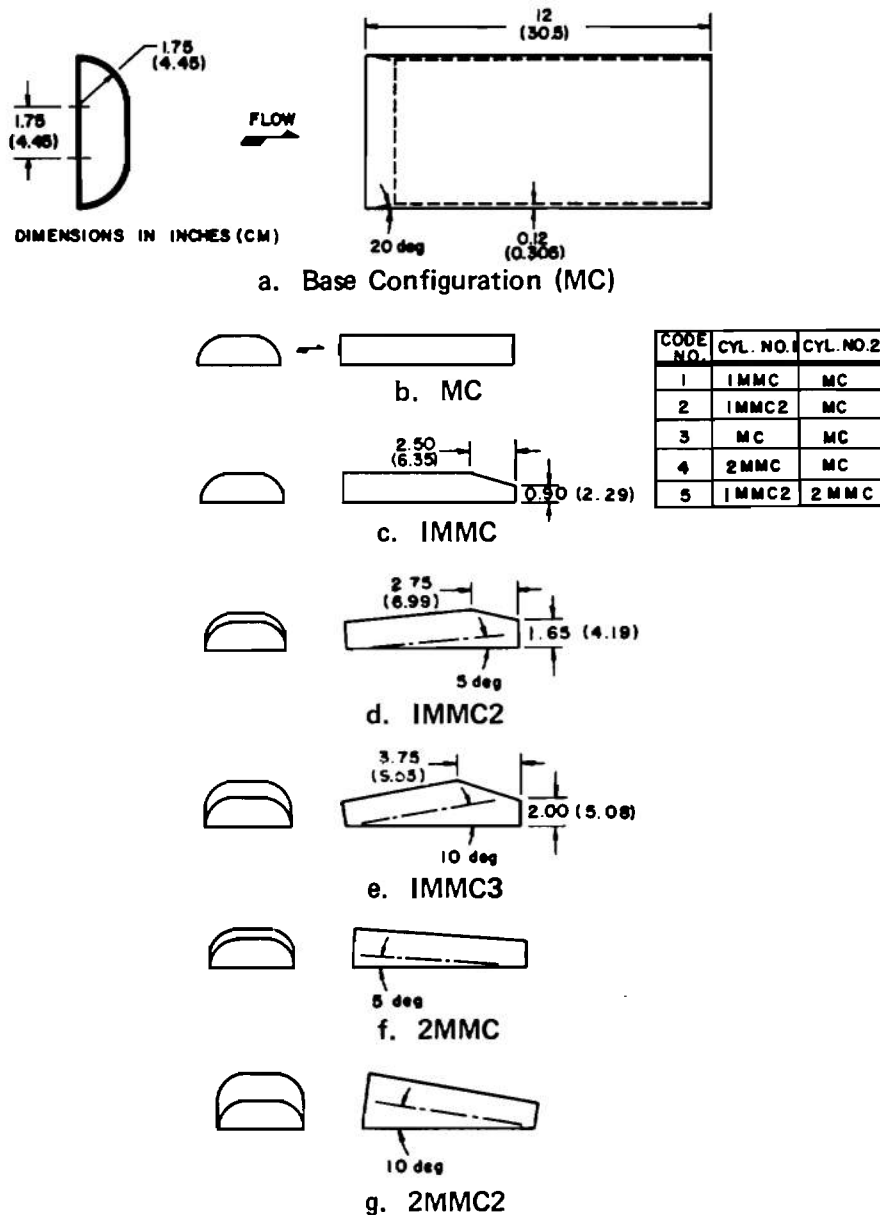


Figure 9. Schematic of flow-shaping device.



Each of the cylinders could be remotely pitched through a continuous angle range from 0 to 35 deg, and the lateral position from the tunnel wall could also be remotely positioned. Both cylinders could be manually yawed relative to the tunnel centerline to +10 or -5 deg. The position of the cylinders shown schematically in Fig. 8 is shown for the actual installation of the cylinders and positioning mechanism in Fig. 10.

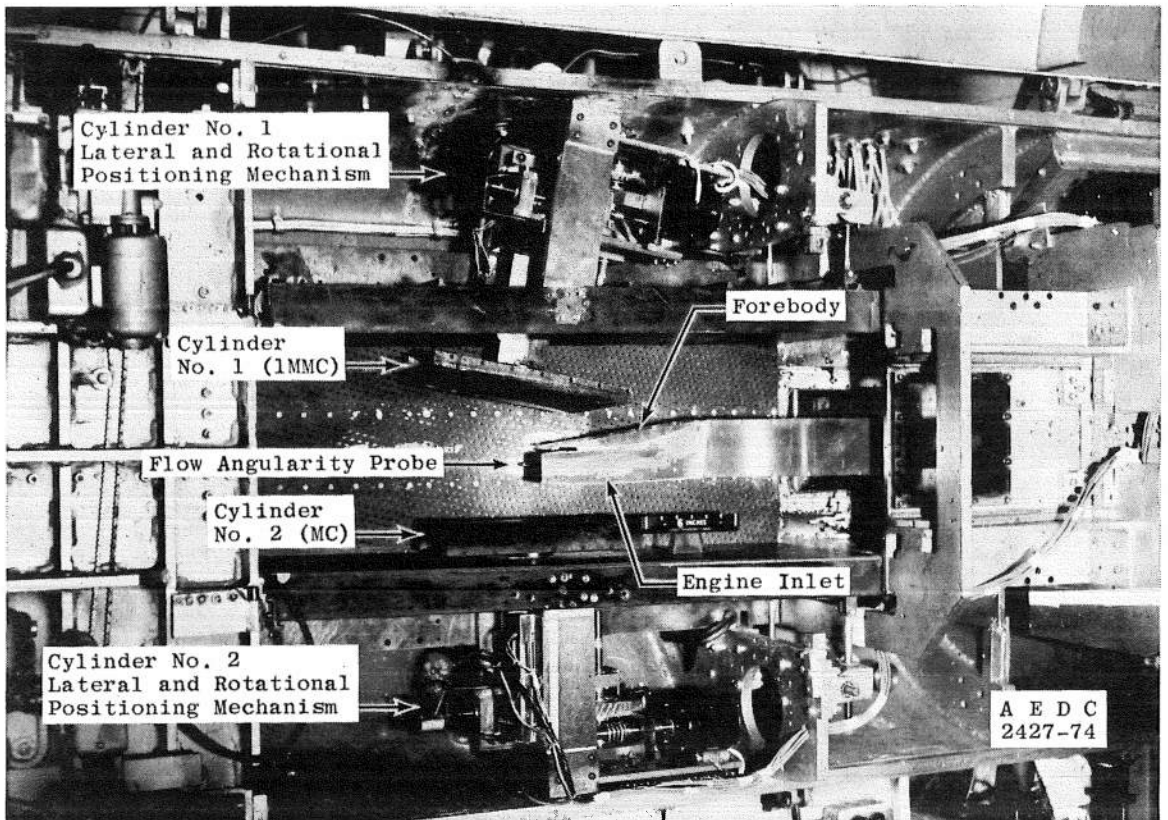


Figure 10. Model and cylinder positioning mechanism installed in PWT-1T.

### 3.5 INSTRUMENTATION AND DATA ACQUISITION SYSTEMS

In the PWT-4T study the model and flow angularity probe pressures were measured using 15-psid transducers. Translational and angular positions of the probe were obtained from the CTS analog outputs. The model angle of attack was set using the main sting support and readout system. The inlet model was instrumented with a touch wire, and the system was electrically wired to give a visual indication on the control console when contact between the probe and touch wire was made. This allowed the probe to be set in an exact location with respect to the inlet for each test condition. The data reduction was performed on the PWT Raytheon 520<sup>®</sup> facility computer.

Tunnel 1T is equipped with a permanently installed, automatic data recording system. A PDP 11-20 computer provides on-line data reduction. Reduced data are displayed on a line printer, and a high-speed paper tape punch records and stores the raw data for the purpose of later off-line analysis. The pressure data are measured with differential pressure transducers referenced to the tunnel plenum pressure. Analog signals from the transducers are fed through a switch gain amplifier and then through an analog-to-digital (A-to-D) converter to be digitized. The A-to-D converter uses 12 bits plus sign or 4096 counts full scale. The digital signal from the converter is processed by the PDP 11-20 computer.

The pressure measurements in both PWT-4T and PWT-1T were accurate to 0.03 psi, and the CTS probe angle was accurate to 0.25 deg.

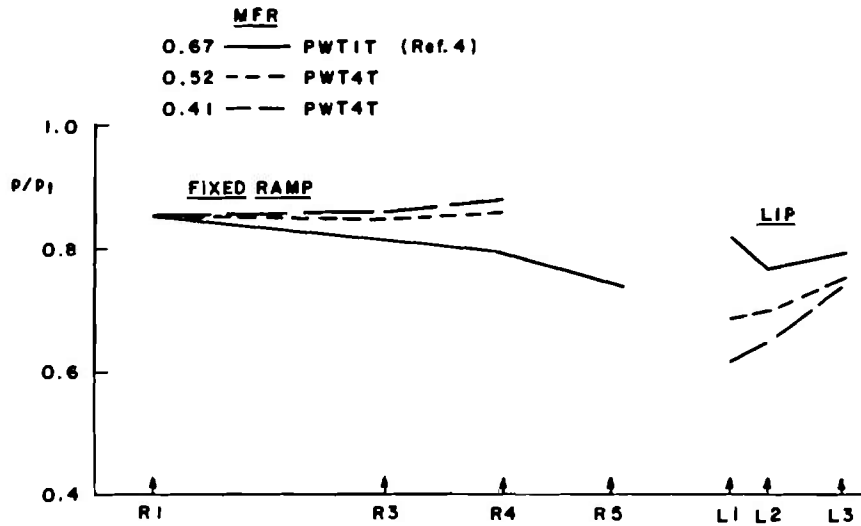
#### 4.0 RESULTS AND DISCUSSION

To verify the new flow-shaping technique for testing full-scale inlet/engine systems at angles of yaw and combinations of angle of attack and yaw, it was first necessary to obtain data on a basic fuselage/inlet model configuration (see Fig. 1) at known geometric pitch angles, yaw angles, and wind tunnel free-stream Mach numbers in PWT-4T.

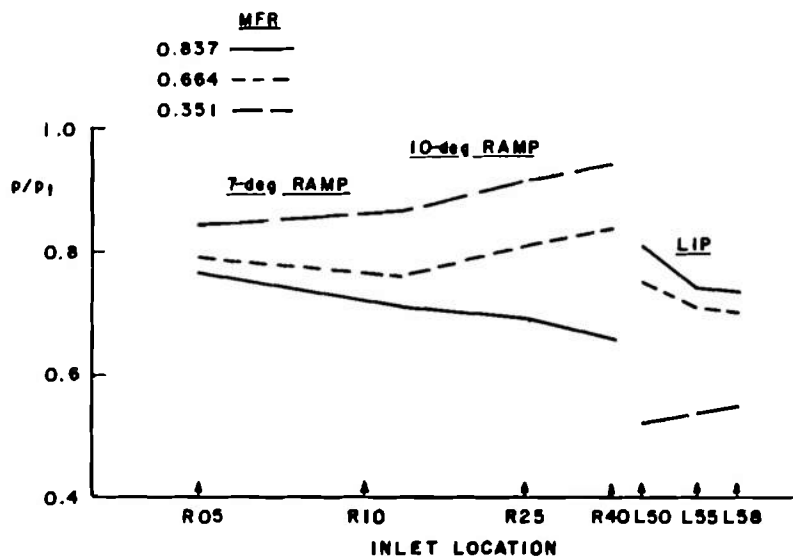
Two problems not anticipated were encountered in obtaining the basic data in PWT-4T. First, the scavenging system was inadequate to produce an inlet mass flow typical of the cruise power mass flow usually obtained during the PWT-1T experiments. As a result the mass flow ratio (MFR) became an additional parameter that had to be duplicated between the PWT-4T base data and the simulation in PWT-1T. To be assured that the effects of mass flow on the performance of the 1/16-scale inlet model were the same as those on a full-scale inlet model, a comparison is made in Fig. 11 of the trends encountered in Tunnels 1T and 4T with those of a full-scale inlet model in PWT-16T. Although the inlet geometries are different (the subscale and full scale are basic two-dimensional, external compression inlets), the basic trends are quite similar. This indicates that a duplication of the MFR is necessary during any simulation of the inlet flow field and that the subscale verification is adequate.

The second problem involved the side loads on the flow angularity probe. These loads were too large for the CTS system at a stagnation pressure which matched the stagnation pressure in PWT-1T, where the simulation study would be made. This forced a reduction in stagnation pressure, which caused a potential problem in Reynolds number mismatch during the simulation study. To assure that the inability to match Reynolds

number between the base data and the simulation data would not cause a discrepancy in the results, data were taken at four different Reynolds numbers at a constant free-stream Mach number and constant MFR in PWT-4T. The comparison of these data is shown in Fig. 12. There was no appreciable effect of Reynolds number on the inlet surface pressure distribution.



a. 0.0625-scale research inlet data from PWT-4T and 1T test ( $MO = 0.6$ ).



b. Large-scale inlet data from PWT-16T test ( $MO = 0.7$ )  
 Figure 11. Effect of changes in MFR on inlet surface pressure distribution at  $\alpha = 0$  and  $\psi = 0$ .

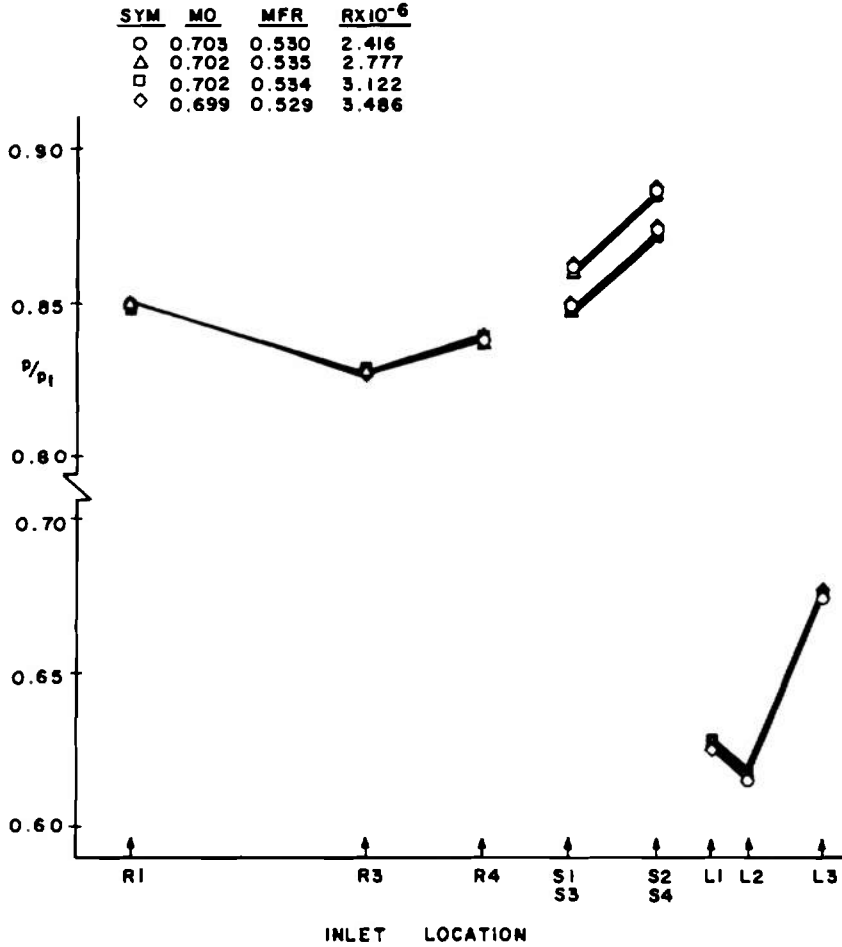


Figure 12. Effect of changes in unit Reynolds number in PWT-4T on the inlet surface pressure distribution at  $\alpha = 4$  deg and  $\psi = -4$  deg.

Base data were obtained during the PWT-4T experiments with the fuselage/inlet model at yaw angles from +6 to -6 deg over an angle-of-attack range from 0 to 20 deg for a range of Mach numbers from 0.6 to 0.9. Flow angularity and local Mach number in front of the inlet along with inlet surface pressure with the probe moved from in front of the inlet were measured at each model attitude and free-stream condition. After the base data had been obtained, the fuselage was removed from the inlet and was replaced with the N-1 forebody (see Fig. 6). The base data were then duplicated by simulating the inlet flow field in PWT-1T using the inlet/N-1 configuration and the flow-shaping devices. Flow angularity, local Mach number, and inlet surface pressure were also measured for each simulation condition.

In setting up a specific condition for simulation, two parameters were manually fixed during tunnel operation, and four parameters were remotely adjustable. The two manually fixed parameters were cylinder yaw angle and inlet pitch angle. The four adjustable parameters were cylinder rotation, cylinder lateral position, inlet mass flow ratio (MFR), and free-stream Mach number. Each of these adjustments had a strong influence on the other, which resulted in use of an iterative process for any one simulation condition. Three of these parameters were easily adjusted; however, the MFR, which was one of the most sensitive parameters, was set with a very insensitive valve.

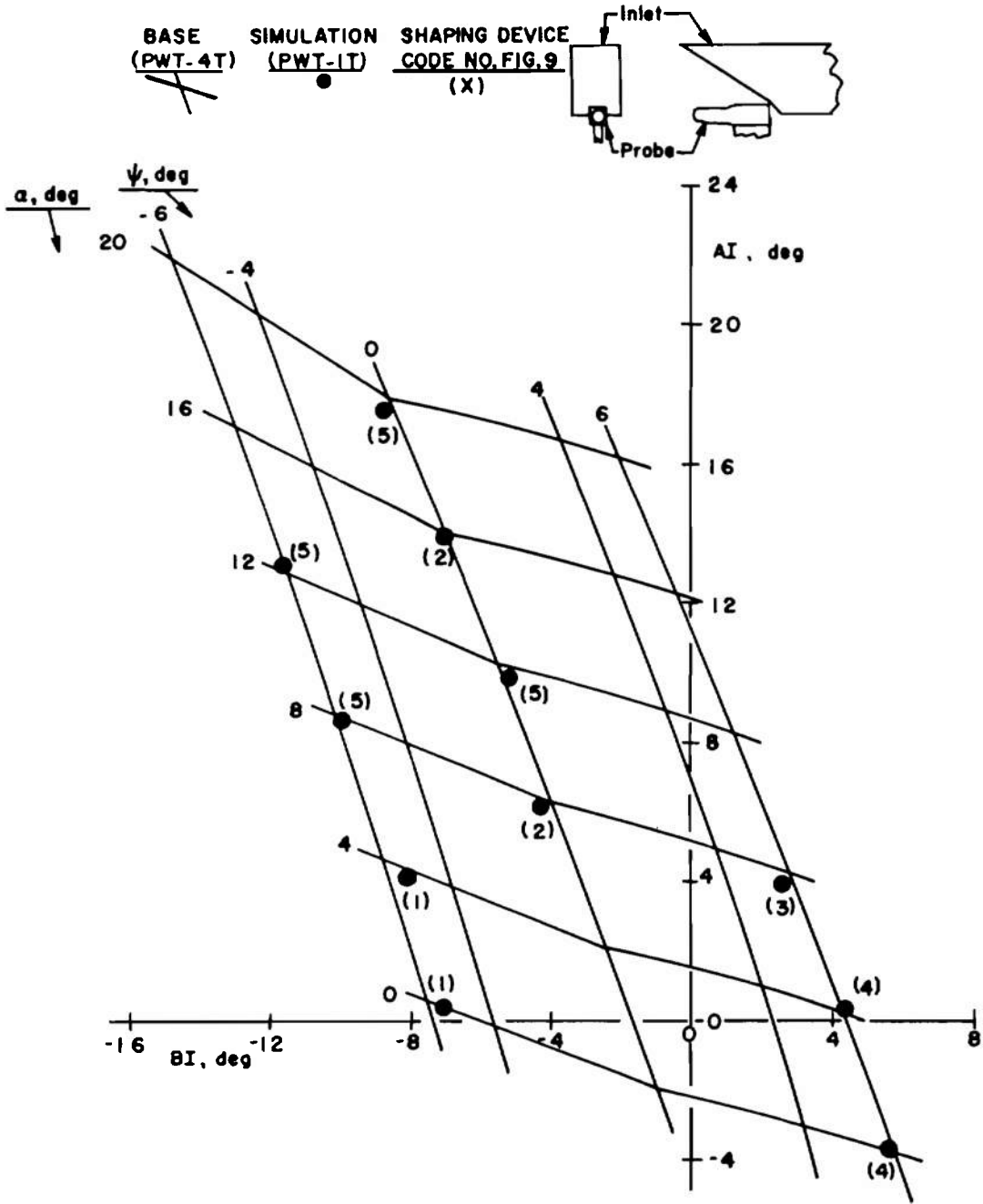
Five combinations of the cylinder configurations were required to cover the complete range of simulation. The cylinder configuration, rotational and lateral position, yaw angle, etc., along with the tunnel conditions for simulation, are given in Table 1.

The local upwash and sidewash angle in front of the inlet from the base data compared with the simulation data are given in Fig. 13. The intersection of the lines indicates the measured flow angles at the particular pitch and yaw angles for the base data. The solid symbols indicate the measured flow angles during simulation. This comparison shows good to excellent agreement between the base data and the simulated data. The number in parentheses designates the shaping device configuration (see Fig. 9) required for the simulation. During the simulation it was found that for a given flow-shaping cylinder yaw condition (for sidewash simulation), as the cylinders are rotated in pitch (for upwash simulation), the induced sidewash effect decreases as the induced upwash effect increases. Since the cylinder pitch rotation point was fixed and the inlet pitch rotation point was fixed, it was difficult to exactly duplicate some conditions. This has no bearing on the accuracy of the data presented in this figure but only means that instead of simulating a -6 deg yaw angle at an angle of attack of 4 deg (Fig. 13a, for example), the actual simulation was for a -5 deg yaw angle at an angle of attack of 4 deg. This will, however, account for the variations in the comparison of the inlet surface pressure made later. A four-degree-of-freedom positioning system for the flow-shaping devices would eliminate this difficulty.

Two points should be noted here. First, the simulation of +6 deg yaw at angles of attack of 4 and 8 deg is not shown for Mach 0.9 because the simulation of the upwash and sidewash was not considered close enough to make a comparison of the inlet surface pressure at these angles. Second, although the simulated -6 deg yaw angle is the highest shown in Fig. 13, sidewash angles were measured at low angles of attack indicating that it might be possible to simulate -15 deg yaw angle at zero angle of attack and -10 deg yaw angle at 4 deg angle of attack. No base data were available for verification of these simulation conditions.

Table 1. Tabulated PWT-1T, Inlet Model, and Shaping Device Settings for Flow Simulation

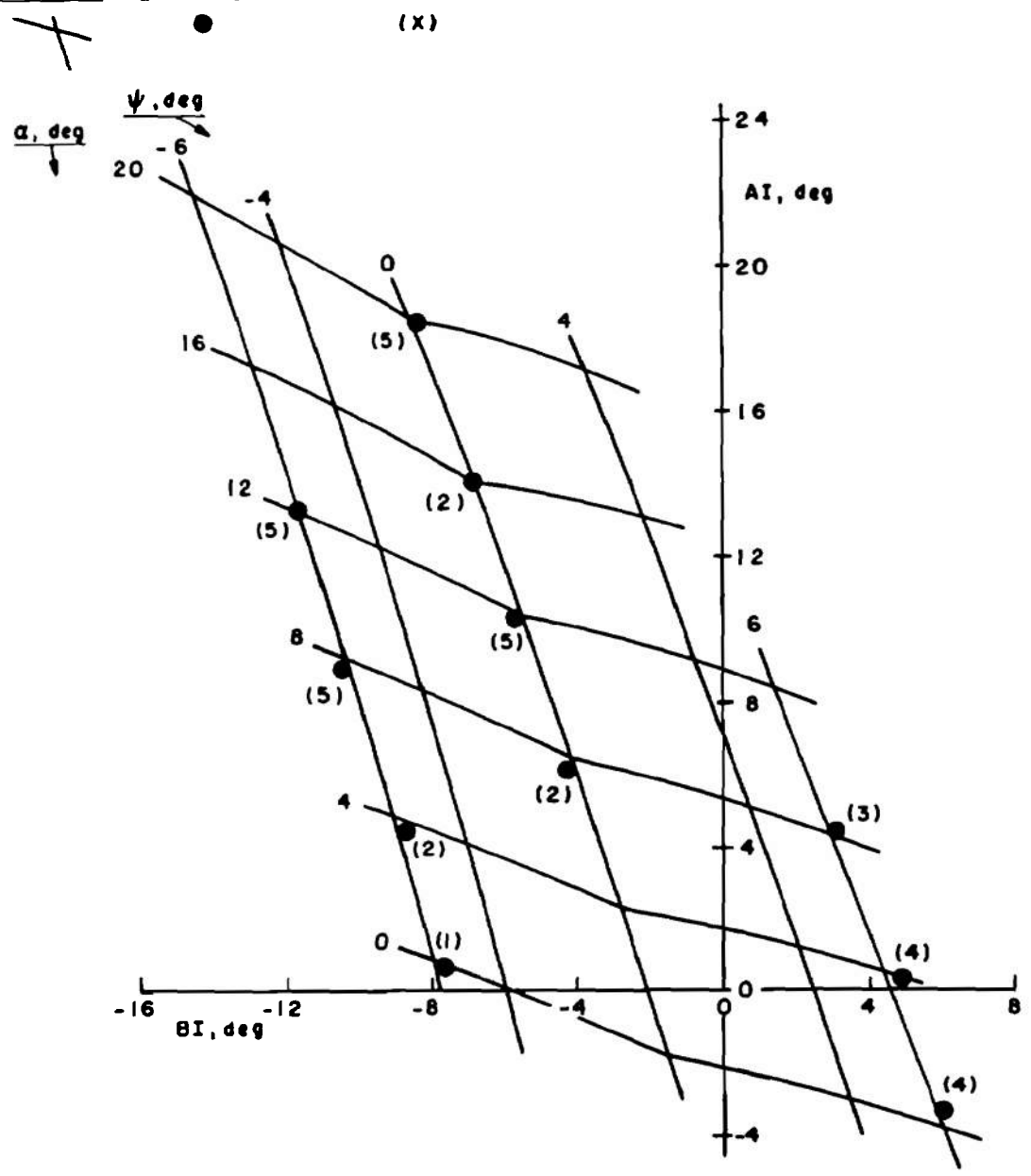
Simulated Flight			PWT-1T Test Condition		Inlet Configuration		Cylinder No. 1 (Top)				Cylinder No. 2 (Bottom)				
Mach No.	$\alpha$ , deg	$\psi$ , deg	MO	$\theta$ , deg	Forebody	$\alpha$ , deg	Code No., Fig. 9	$\alpha_s$ , deg	$\beta$ , deg	LP, in. (cm)	Code No., Fig. 9	$\alpha_s$ , deg	$\beta$ , deg	LP, in. (cm)	
0.6	0	-6	0.62	1	N-1	2	1MMC	6.0	10	2.2 (5.59)	MC	6.1	-5	0.9 (2.29)	
	4	↓	0.62	↓		2	1MMC	15.0	↓	2.5 (6.35)	MC	15.1	↓	↓	
	8	↓	0.58	↓		6	1MMC2	9.1	↓	2.8 (7.11)	2MMC	9.0	↓	↓	
	12	↓	0.52	↓		10	1MMC2	6.0	↓	2.4 (6.10)	2MMC	6.0	↓	↓	
	0	6	0.57	↓		2	2MMC	-18.0	0	2.2 (5.59)	MC	-18.0	5	0.7 (1.78)	
	4	6	0.61	↓		2	2MMC	6.9	0	0.7 (1.78)	MC	7.0	5	0.7 (1.78)	
	8	6	0.60	↓		2	MC	18.0	0	2.4 (6.10)	MC	18.0	5	0.7 (1.78)	
	12	0	0.58	↓		8	1MMC2	11.4	10	2.3 (5.84)	2MMC	11.7	0	0.4 (1.02)	
	16	0	0.56	↓		6	1MMC2	22.4	↓	2.6 (6.60)	MC	22.4	-5	0.9 (2.29)	
	20	0	0.50	↓		8	1MMC2	19.0	↓	2.8 (7.11)	2MMC	19.0	↓	↓	
	0.7	0	-6	0.74		↓	2	1MMC	8.1	↓	2.4 (6.10)	MC	8.2	↓	↓
		4	↓	0.73		↓	2	1MMC2	15.0	↓	2.6 (6.60)	MC	15.0	↓	↓
		8	↓	0.70		↓	6	1MMC2	9.0	↓	2.8 (7.11)	2MMC	9.0	↓	↓
		12	↓	0.61		↓	10	1MMC2	6.0	↓	2.2 (5.59)	2MMC	6.0	↓	↓
		0	6	0.67		↓	2	2MMC	-15.0	0	2.1 (5.33)	MC	-15.0	5	0.7 (1.78)
		4	6	0.70		↓	2	2MMC	6.9	0	0.7 (1.78)	MC	7.0	5	0.7 (1.78)
8		6	0.74	↓	2	2MMC	19.1	0	2.4 (6.10)	MC	19.1	5	0.7 (1.78)		
12		0	0.67	↓	4	1MMC2	20.0	10	2.1 (5.33)	2MMC	20.0	-5	0.9 (2.29)		
16		0	0.62	↓	6	1MMC2	22.4	↓	2.6 (6.60)	MC	22.4	↓	0.9 (2.29)		
20		0	0.55	↓	8	1MMC2	16.9	↓	2.2 (5.59)	2MMC	16.9	↓	0.9 (2.29)		
0.8		0	-6	0.82	↓	2	1MMC	6.0	↓	2.3 (5.84)	MC	6.0	↓	0.9 (2.29)	
		4	↓	0.82	↓	2	1MMC	15.9	↓	2.6 (6.60)	MC	16.0	↓	↓	
		8	↓	0.80	↓	6	1MMC2	10.0	↓	2.8 (7.11)	2MMC	9.9	↓	↓	
		12	↓	0.70	↓	10	1MMC2	6.4	↓	2.2 (5.59)	2MMC	6.4	↓	↓	
		0	6	0.74	↓	2	2MMC	-17.2	0	2.4 (6.10)	MC	-17.2	5	0.7 (1.78)	
		4	6	0.83	↓	2	2MMC	7.2	0	0.7 (1.78)	MC	7.0	5	0.7 (1.78)	
	8	6	0.88	↓	2	MC	19.1	0	2.4 (6.10)	MC	19.1	5	0.7 (1.78)		
	12	0	0.79	↓	4	1MMC2	20.0	10	1.4 (3.56)	2MMC	20.0	-5	0.9 (2.29)		
	16	0	0.74	↓	6	1MMC2	18.9	↓	1.5 (3.81)	2MMC	18.9	↓	↓		
	20	0	0.63	↓	6	1MMC2	29.0	↓	2.9 (7.37)	2MMC	29.0	↓	↓		
	0.9	0	-6	0.90	↓	2	1MMC	6.0	↓	2.3 (5.84)	MC	6.0	↓	↓	
		4	↓	0.92	↓	2	1MMC2	16.1	↓	2.6 (6.60)	MC	16.0	↓	↓	
		8	↓	0.91	↓	6	1MMC2	9.0	↓	2.8 (7.11)	2MMC	8.9	↓	↓	
		12	↓	0.77	↓	10	1MMC2	6.5	↓	1.7 (4.32)	2MMC	6.4	↓	↓	
		0	6	0.85	↓	2	2MMC2	-14.2	0	2.2 (5.59)	MC	-14.2	5	0.7 (1.78)	
		12	0	0.77	↓	2	1MMC2	32.2	10	1.8 (4.57)	MC	32.1	-5	0.9 (2.29)	
16		0	0.84	↓	6	1MMC2	18.9	10	1.7 (4.32)	2MMC	18.9	-5	0.9 (2.29)		



a. MO = 0.6

Figure 13. Local upwash and sidewash angles in front of the inlet as a function of aircraft pitch and yaw angles.

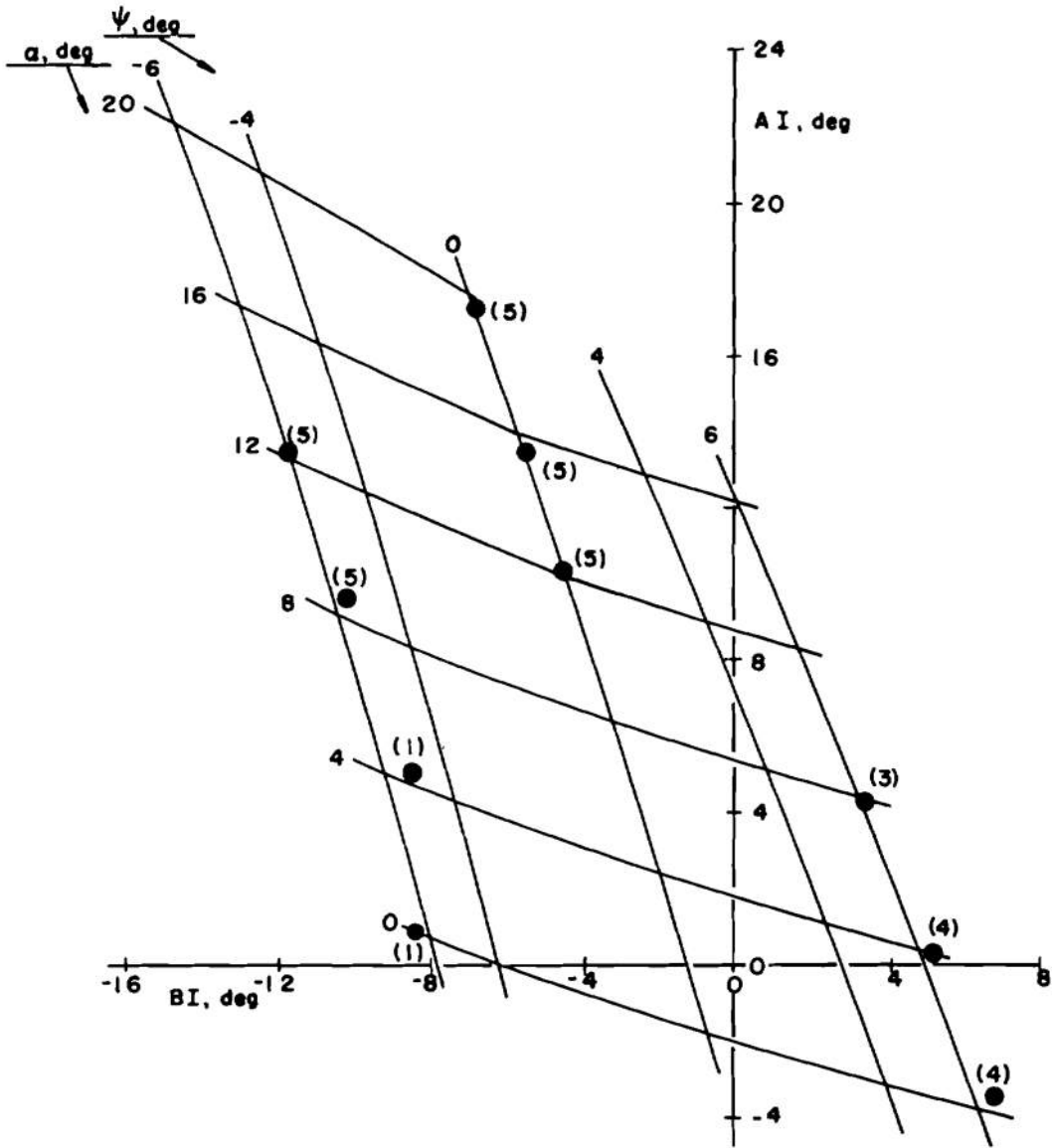
BASE (PWT-4T)    SIMULATION (PWT-1T)    SHAPING DEVICE (X)  
 CODE NO. FIG. 9



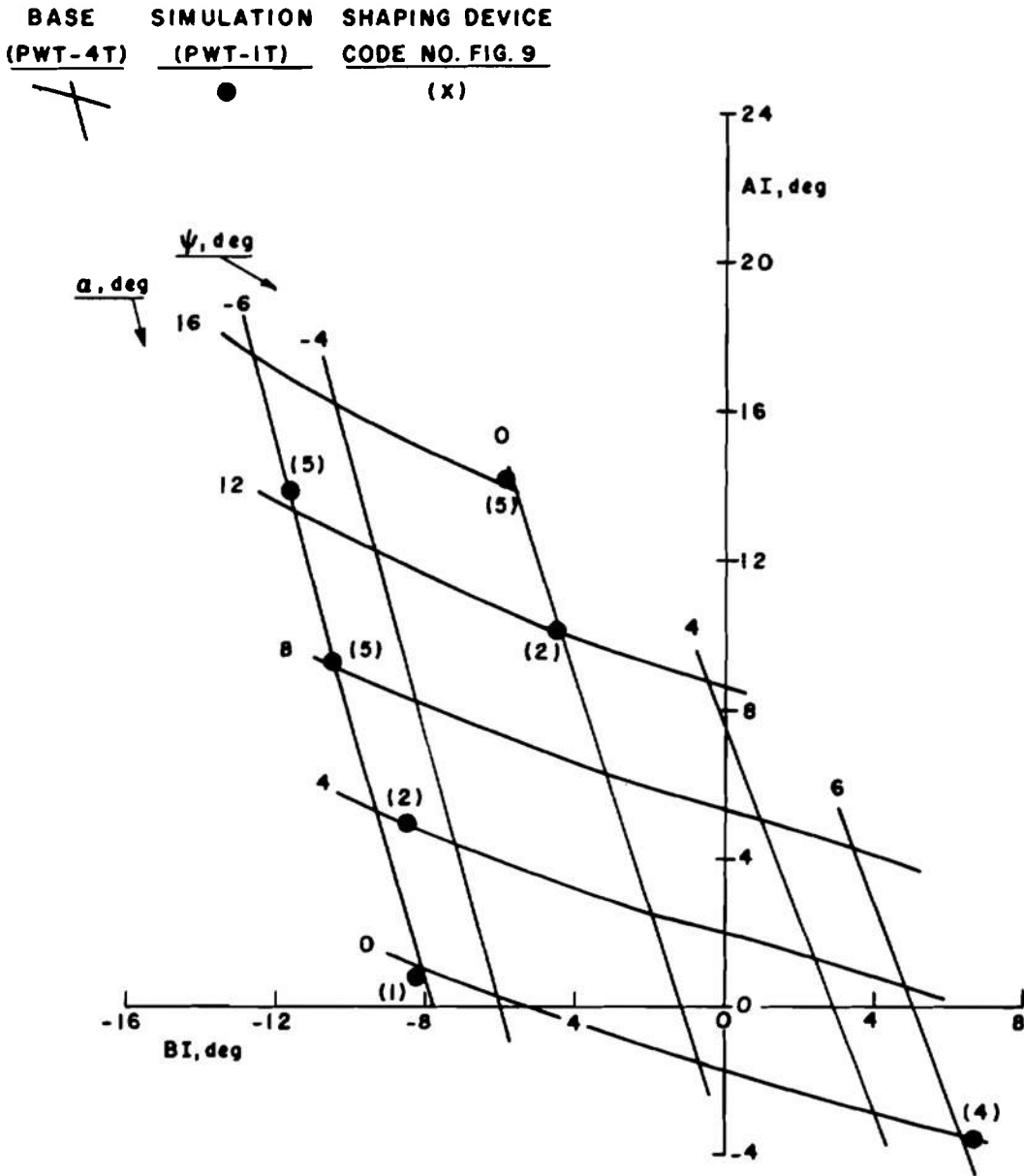
b. MO = 0.7  
 Figure 13. Continued.



BASE SIMULATION SHAPING DEVICE  
 (PWT-4T) (PWT-1T) CODE NO. FIG. 9  
 (X)



c. MO = 0.8  
 Figure 13. Continued.



d.  $MO = 9$   
Figure 13. Concluded.

The local Mach number in front of the inlet is shown in Fig. 14. For the most part, the local Mach number simulation was good and the adjustment of this parameter presented no problems. This parameter was adjusted by adjusting the tunnel free-stream Mach number. The differences are due not to interference but to failure to adjust the Mach number after adjustments were made to the other variables.

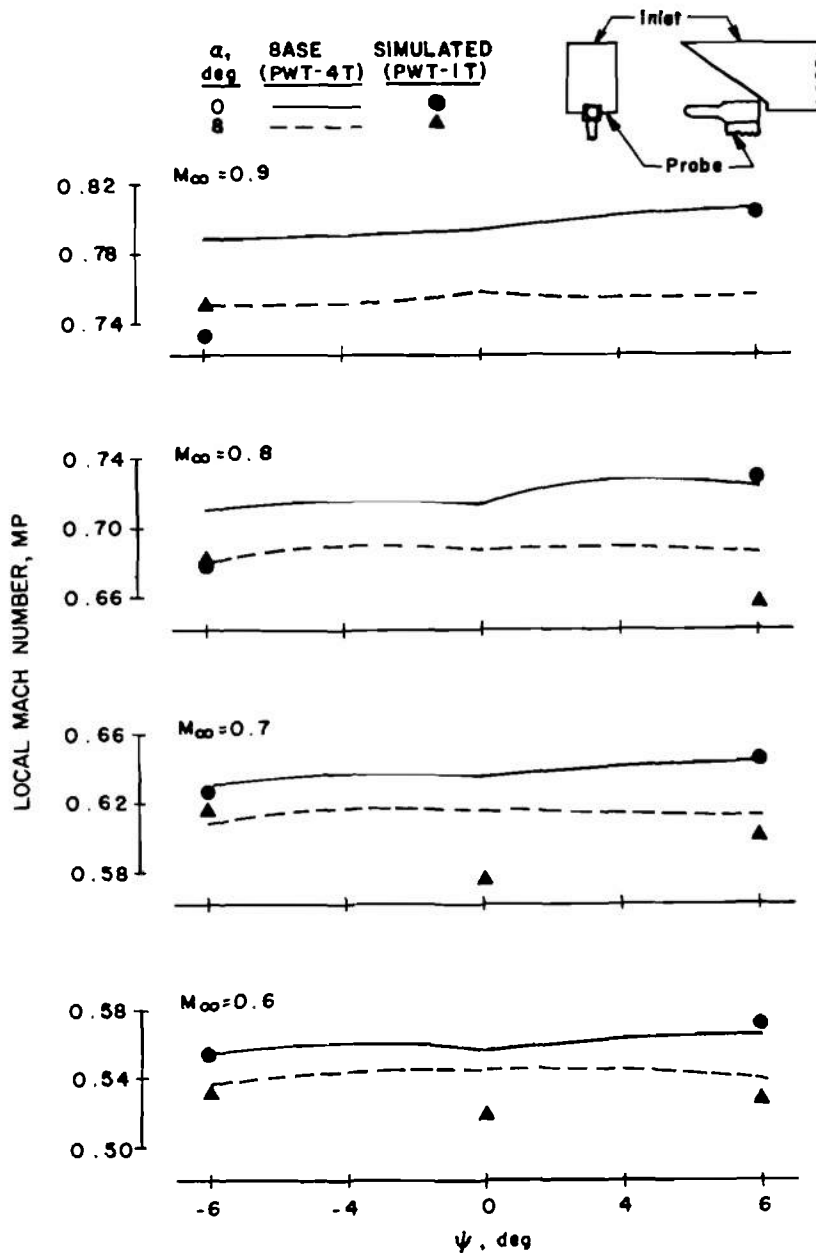


Figure 14. Local Mach number in front of the inlet as a function of aircraft pitch and yaw angles.

The comparison of the inlet surface pressure distribution for the geometric and simulated yaw and pitch-yaw combinations is shown in Figs. 15, 16, 17, and 18. The main concern was simulation of the sideplate pressure (S1-4), which should be the most sensitive to yaw angle. These data show excellent agreement in the sideplate pressure;

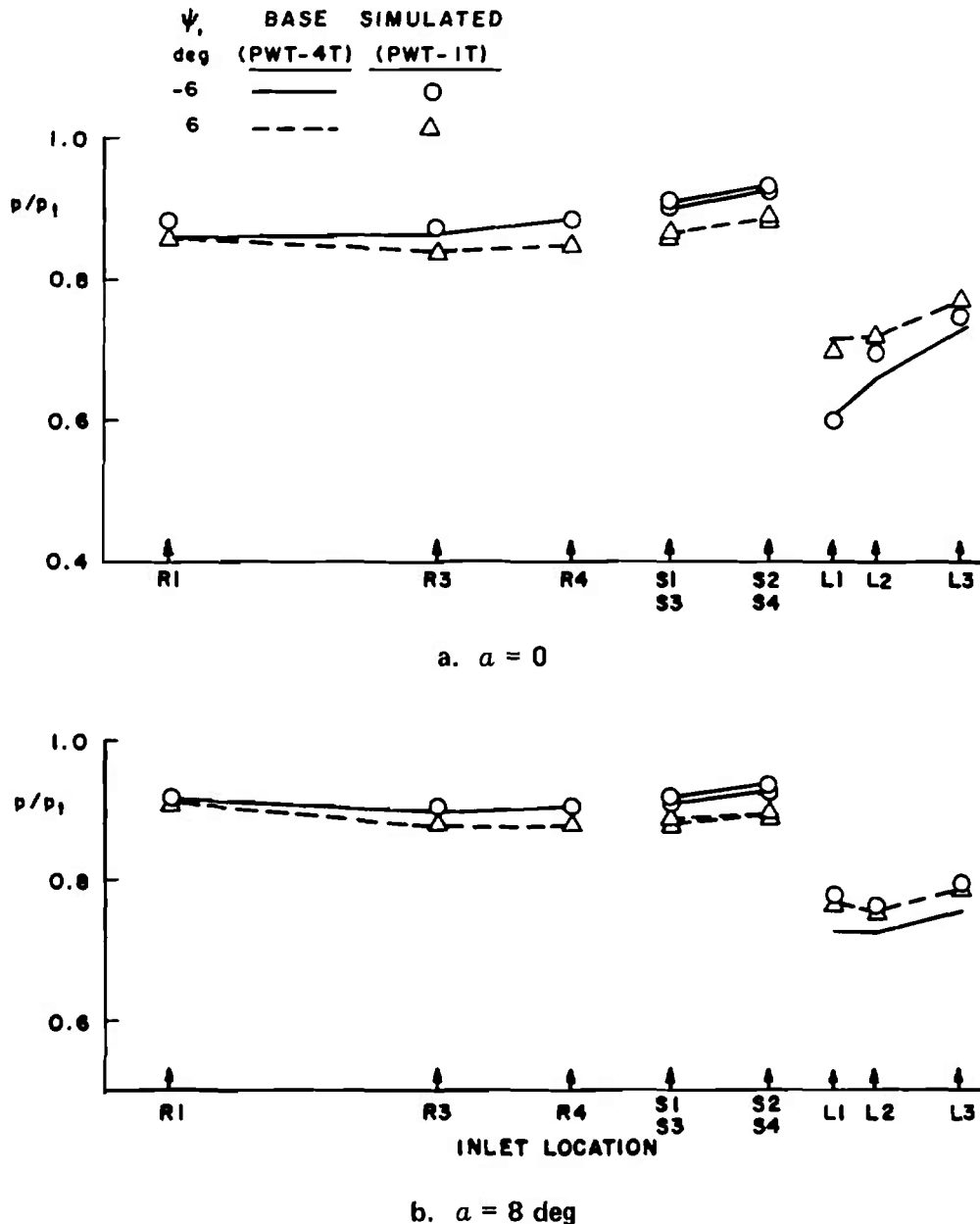


Figure 15. Comparison of inlet surface pressure distribution for actual and simulated yaw and pitch-yaw combinations at a Mach number of 0.6.

however, the lip pressure was not as good in some cases. The lip pressure seemed to be extremely sensitive to MFR at the low MFR settings required to match the base data MFR. The difficulty in setting MFR coupled with the fixed rotation point problem (discussed earlier), which caused the lip to move out of the desired location with respect to the cylinders, accounts for the discrepancies in the data match of the lip pressure.

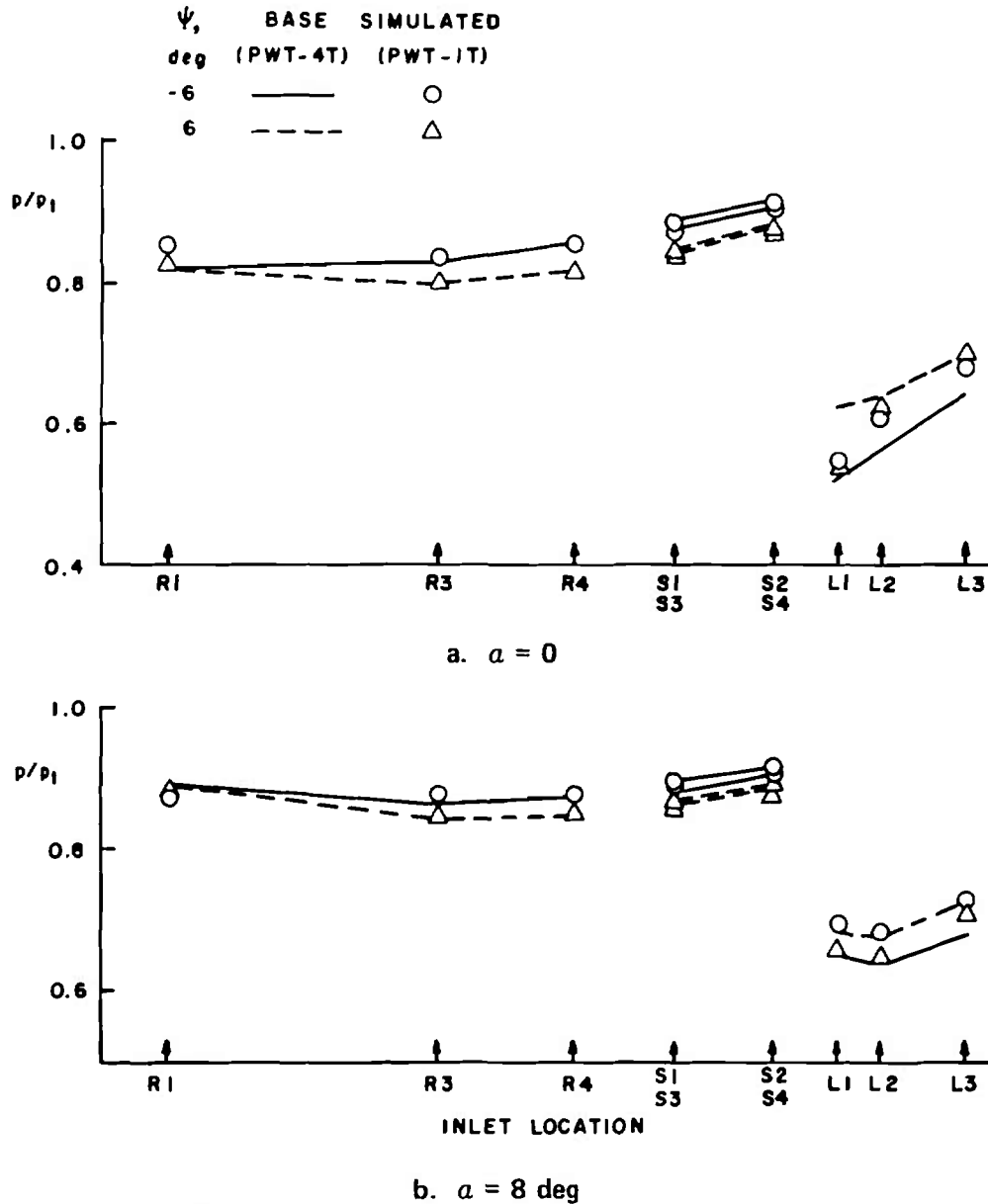
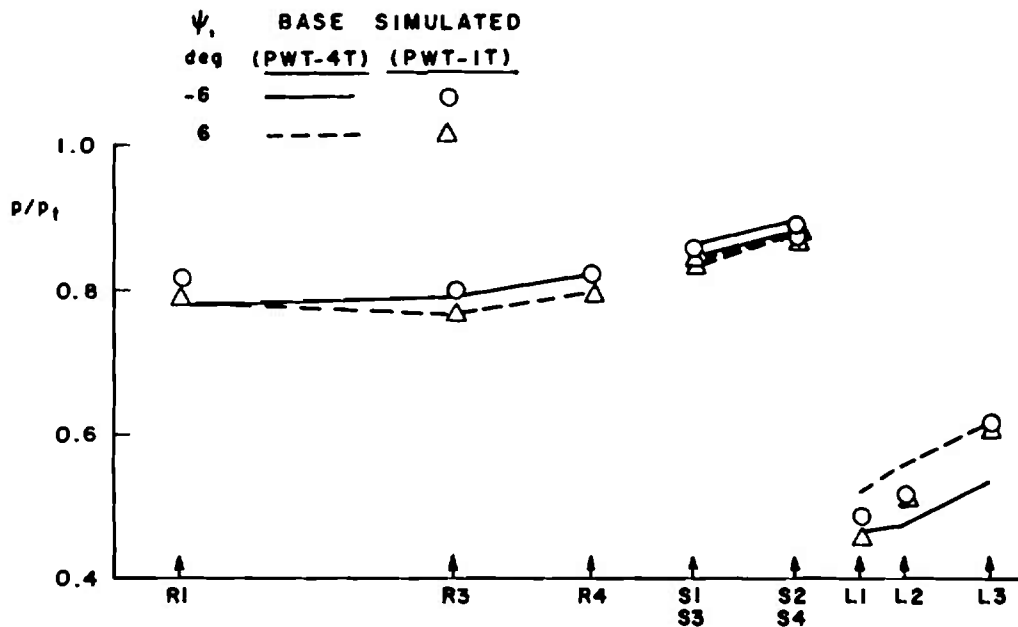
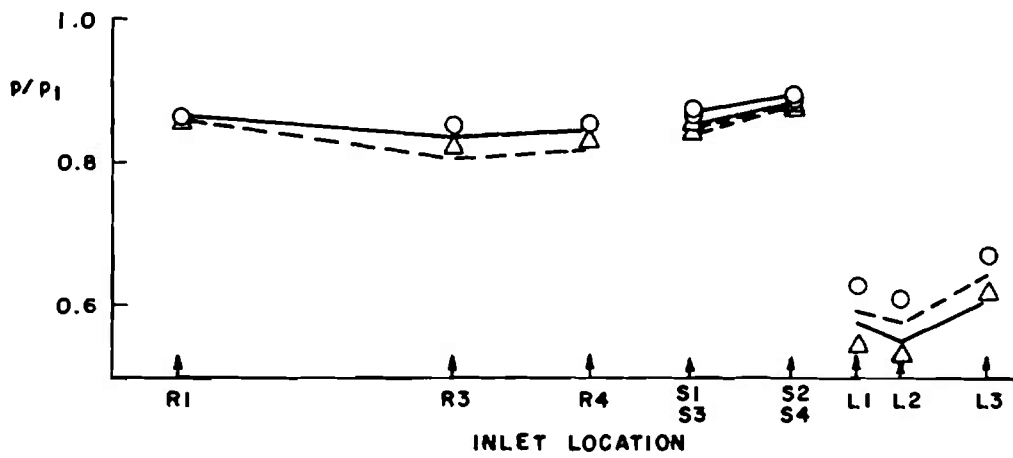


Figure 16. Comparison of inlet surface pressure distribution for actual and simulated yaw and pitch-yaw combinations at a Mach number of 0.7.

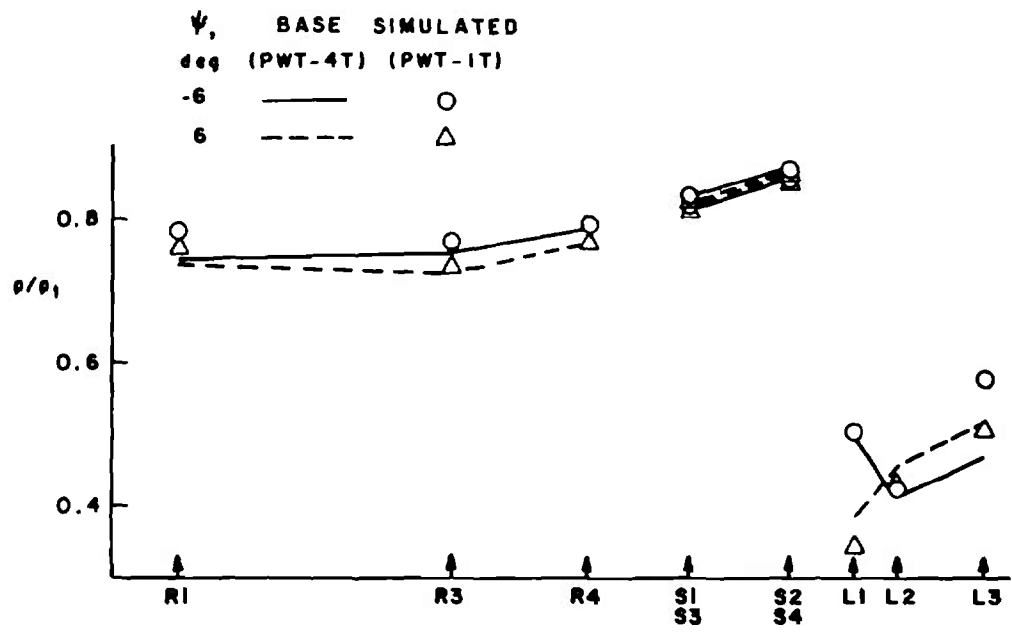


a.  $\alpha = 0$

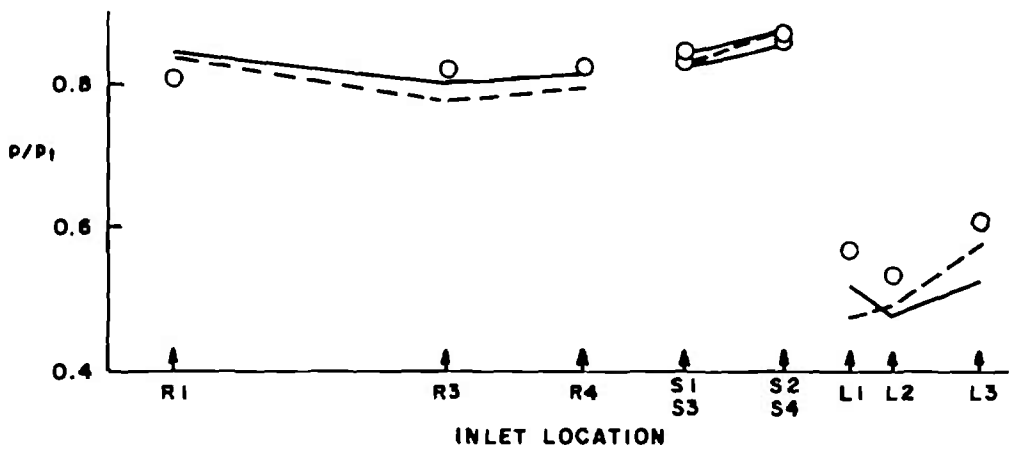


b.  $\alpha = 8$  deg

Figure 17. Comparison of inlet surface pressure distribution for actual and simulated yaw and pitch-yaw combinations at a Mach number of 0.8.



a.  $\alpha = 0$



b.  $\alpha = 8$  deg

Figure 18. Comparison of inlet surface pressure distribution for actual and simulated yaw and pitch-yaw combinations at a Mach number of 0.9.

Simulation of the high angle-of-attack data at zero yaw was also made. Typical of this simulation effort is the data shown in Fig. 19. Here, as in the yaw simulation, the

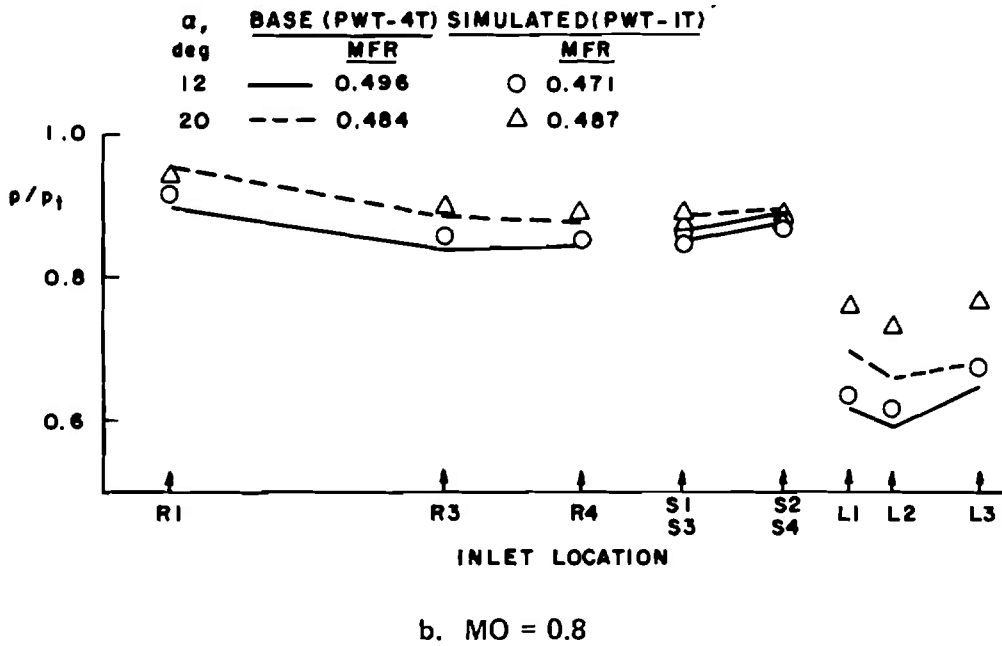
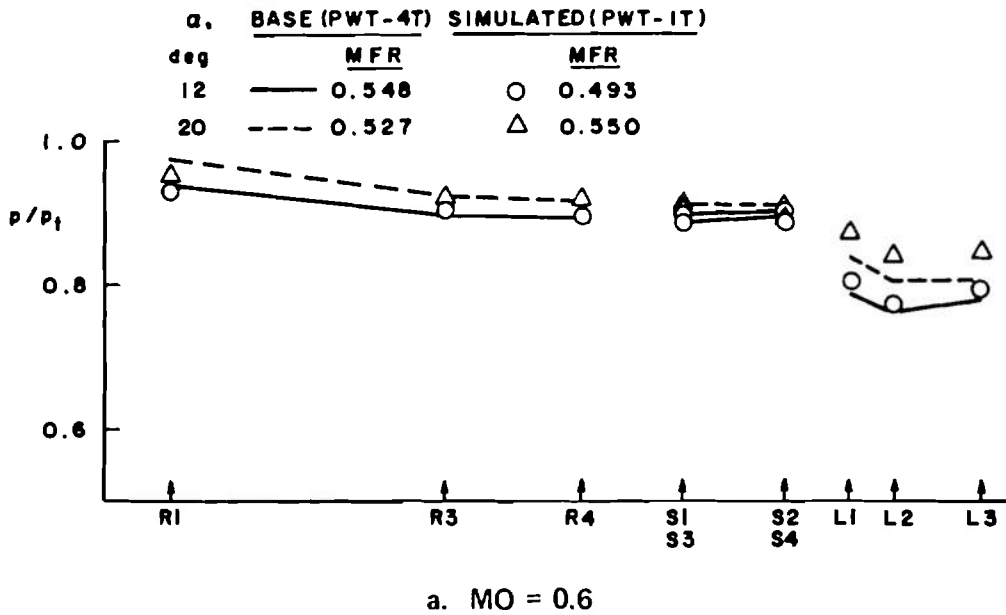


Figure 19. Comparison of inlet surface pressure distribution for actual and simulated pitch angles.



lip pressure does not compare as well as desired, and for the same reasons. Figure 20 shows the effect of increasing the MFR for the same pitch-yaw simulation. The solid symbols represent the high MFR data. These high MFR data compare well with the same simulation angles and MFR in Ref. 4.

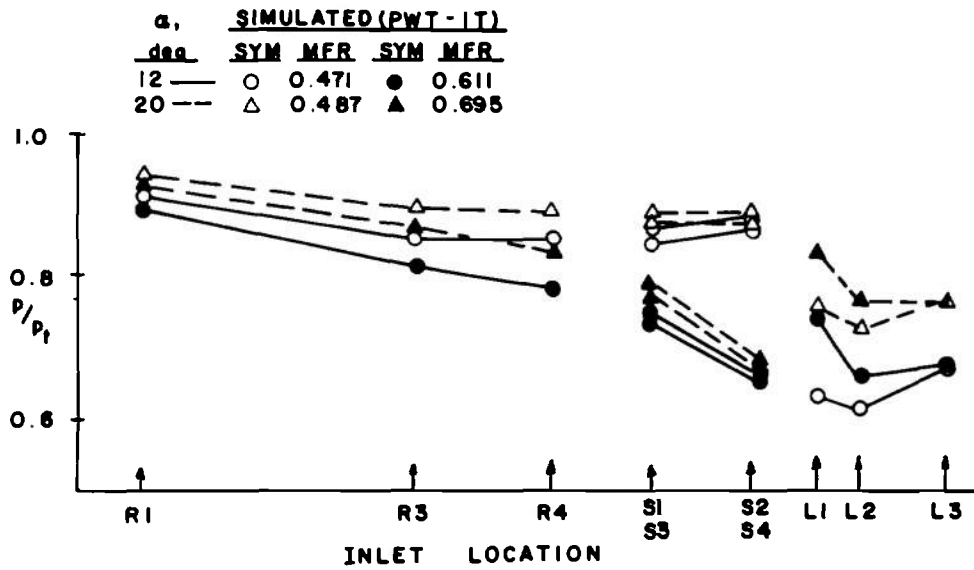
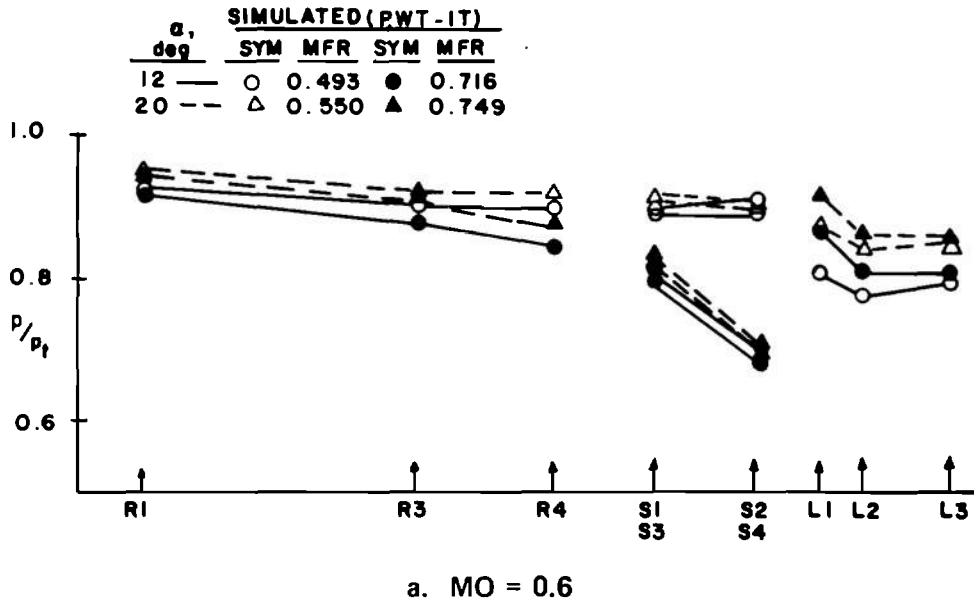


Figure 20. Effect of change in MFR on inlet surface pressure distribution.

The aircraft maneuvering requirements, present testing capability (in PWT-16T), project objective, and project achievement are shown in Fig. 21.

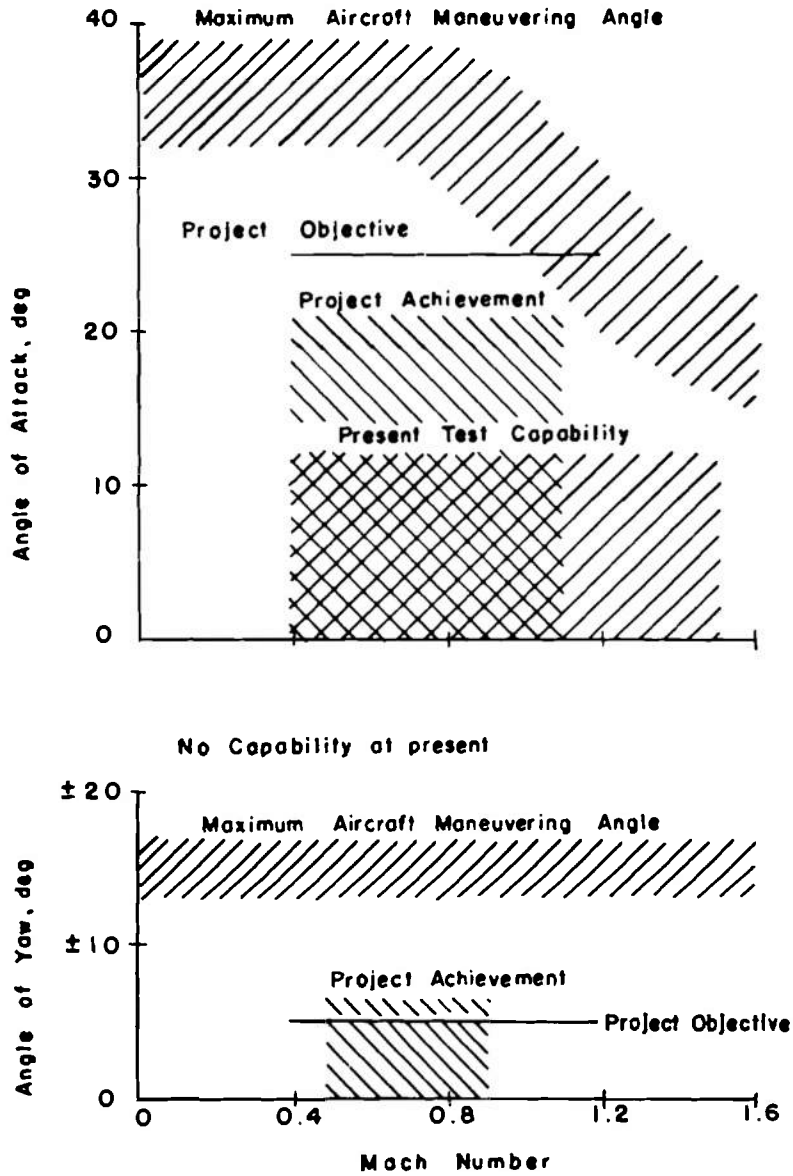


Figure 21. Typical performance for highly maneuverable aircraft and full-scale inlet/engine testing capability of the AEDC 16-ft Transonic Wind Tunnel.

## 5.0 CONCLUDING REMARKS

Experimental verification of the flow-shaping technique for extending the full-scale inlet/engine testing capability of the AEDC PWT-16T to include simulation of maneuvering conditions has been accomplished. Simulation of 6-deg yaw angle at angles of attack from 0 to 8 deg and of -6 deg yaw angle at angles of attack from 0 to 12 deg has been shown in this report. The ability to duplicate the upwash and sidewash angles and the local Mach number in front of the inlet has been demonstrated. The requirement for a minimum of four degrees of freedom in the shaping device positioning system was again demonstrated.

The investigation showed that over the range of simulated conditions tested the flow-shaping technique would significantly increase the present capability of testing full-scale inlet/engine models in the AEDC PWT-16T facility.

## REFERENCES

1. Palko, R. L. "Full-Scale Inlet/Engine Testing at High Maneuvering Angles at Transonic Velocities." AIAA Paper No. 72-1026. Presented at the AIAA Seventh Aerodynamics Testing Conference, Palo Alto, California, September 13-15, 1972.
2. Palko, R. L. "A Method of Testing Full-Scale Inlet/Engine Systems at High Angles of Attack and Yaw at Transonic Velocities." AIAA Paper No. 72-1097. Presented at the AIAA/SAE 8th Joint Propulsion Specialist Conference, New Orleans, Louisiana, November 29-December 1, 1972.
3. Palko, R. L. "A Method to Increase the Full-Scale Inlet/Engine System Testing Capability of the AEDC 16-ft Transonic Wind Tunnel." AEDC-TR-73-9 (AD762912), June 1973.
4. Palko, R. L. "Experimental Verification of a Technique for Testing Full-Scale Inlet/Engine Systems at Angles of Attack up to 20 deg at Transonic Speeds." AEDC-TR-73-169 (AD769307), October 1973.

## NOMENCLATURE

AI	Upwash angle, deg
BI	Sidewash angle, deg
LP	Shaping device lateral position measured from wind tunnel wall, Fig. 8
Lx	Inlet lip orifice designation ( $x = 1, 2, \text{ and } 3$ ), Fig. 6
MFR	Inlet mass flow ratio (actual mass flow/capture area mass flow)
MO	Free-stream Mach number
MP	Local Mach number from flow angularity probe
N-x	Forebody configuration designation ( $x = 1 \text{ and } 2$ )
$p/p_t$	Ratio of inlet surface static pressure to free-stream total pressure
Rx	Inlet ramp orifice designation ( $x = 1, 3, 4, \text{ and } 5$ ), Fig. 6
Sx	Inlet side orifice designation ( $x = 1, 2, 3, \text{ and } 4$ ), Fig. 6
$\alpha$	Inlet angle of attack, deg
$\alpha_s$	Shaping device angle of rotation relative to wind tunnel centerline, deg, Fig. 8
$\beta$	Shaping device angle of yaw relative to wind tunnel centerline, deg, Fig. 8
$\psi$	Inlet angle of yaw, deg